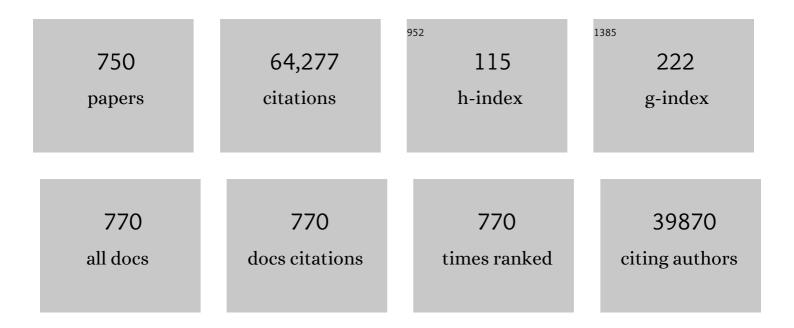
## Aiqin Wang

List of Publications by Year in descending order

Source: https://exaly.com/author-pdf/7163802/publications.pdf Version: 2024-02-01



#	Article	IF	CITATIONS
1	Single-atom catalysis of CO oxidation using Pt1/FeOx. Nature Chemistry, 2011, 3, 634-641.	13.6	5,149
2	Single-Atom Catalysts: A New Frontier in Heterogeneous Catalysis. Accounts of Chemical Research, 2013, 46, 1740-1748.	15.6	3,405
3	Heterogeneous single-atom catalysis. Nature Reviews Chemistry, 2018, 2, 65-81.	30.2	2,728
4	Catalytic Transformation of Lignin for the Production of Chemicals and Fuels. Chemical Reviews, 2015, 115, 11559-11624.	47.7	2,200
5	Photoelectrochemical devices for solar water splitting – materials and challenges. Chemical Society Reviews, 2017, 46, 4645-4660.	38.1	1,140
6	FeOx-supported platinum single-atom and pseudo-single-atom catalysts for chemoselective hydrogenation of functionalized nitroarenes. Nature Communications, 2014, 5, 5634.	12.8	890
7	Selective Hydrogenation over Supported Metal Catalysts: From Nanoparticles to Single Atoms. Chemical Reviews, 2020, 120, 683-733.	47.7	871
8	Remarkable Performance of Ir <sub>1</sub> /FeO <sub><i>x</i></sub> Single-Atom Catalyst in Water Gas Shift Reaction. Journal of the American Chemical Society, 2013, 135, 15314-15317.	13.7	811
9	Discriminating Catalytically Active FeN <sub><i>x</i></sub> Species of Atomically Dispersed Fe–N–C Catalyst for Selective Oxidation of the C–H Bond. Journal of the American Chemical Society, 2017, 139, 10790-10798.	13.7	738
10	Direct Catalytic Conversion of Cellulose into Ethylene Glycol Using Nickelâ€Promoted Tungsten Carbide Catalysts. Angewandte Chemie - International Edition, 2008, 47, 8510-8513.	13.8	671
11	Single-atom dispersed Co–N–C catalyst: structure identification and performance for hydrogenative coupling of nitroarenes. Chemical Science, 2016, 7, 5758-5764.	7.4	571
12	Ag Alloyed Pd Single-Atom Catalysts for Efficient Selective Hydrogenation of Acetylene to Ethylene in Excess Ethylene. ACS Catalysis, 2015, 5, 3717-3725.	11.2	545
13	Thermally stable single atom Pt/m-Al2O3 for selective hydrogenation and CO oxidation. Nature Communications, 2017, 8, 16100.	12.8	545
14	Single-Atom Catalysts Based on the Metal–Oxide Interaction. Chemical Reviews, 2020, 120, 11986-12043.	47.7	486
15	Adsorption characteristics of Congo Red onto the chitosan/montmorillonite nanocomposite. Journal of Hazardous Materials, 2007, 147, 979-985.	12.4	428
16	Ultrastable single-atom gold catalysts with strong covalent metal-support interaction (CMSI). Nano Research, 2015, 8, 2913-2924.	10.4	422
17	One-Pot Conversion of Cellulose to Ethylene Glycol with Multifunctional Tungsten-Based Catalysts. Accounts of Chemical Research, 2013, 46, 1377-1386.	15.6	420
18	Magnetic, Durable, and Superhydrophobic Polyurethane@Fe <sub>3</sub> O <sub>4</sub> @SiO <sub>2</sub> @Fluoropolymer Sponges for Selective Oil Absorption and Oil/Water Separation. ACS Applied Materials & Interfaces, 2015, 7, 4936-4946.	8.0	407

#	Article	IF	CITATIONS
19	Atomically dispersed nickel as coke-resistant active sites for methane dry reforming. Nature Communications, 2019, 10, 5181.	12.8	398
20	Highly Efficient Catalysis of Preferential Oxidation of CO in H <sub>2</sub> -Rich Stream by Gold Single-Atom Catalysts. ACS Catalysis, 2015, 5, 6249-6254.	11.2	380
21	Recent Advances in Preferential Oxidation of CO Reaction over Platinum Group Metal Catalysts. ACS Catalysis, 2012, 2, 1165-1178.	11.2	378
22	Hydroformylation of Olefins by a Rhodium Singleâ€Atom Catalyst with Activity Comparable to RhCl(PPh <sub>3</sub> ) <sub>3</sub> . Angewandte Chemie - International Edition, 2016, 55, 16054-16058.	13.8	376
23	Performance of Cu-Alloyed Pd Single-Atom Catalyst for Semihydrogenation of Acetylene under Simulated Front-End Conditions. ACS Catalysis, 2017, 7, 1491-1500.	11.2	374
24	pH-sensitive sodium alginate/poly(vinyl alcohol) hydrogel beads prepared by combined Ca2+ crosslinking and freeze-thawing cycles for controlled release of diclofenac sodium. International Journal of Biological Macromolecules, 2010, 46, 517-523.	7.5	369
25	One-pot catalytic hydrocracking of raw woody biomass into chemicals over supported carbide catalysts: simultaneous conversion of cellulose, hemicellulose and lignin. Energy and Environmental Science, 2012, 5, 6383-6390.	30.8	358
26	PdZn Intermetallic Nanostructure with Pd–Zn–Pd Ensembles for Highly Active and Chemoselective Semi-Hydrogenation of Acetylene. ACS Catalysis, 2016, 6, 1054-1061.	11.2	334
27	Synthesis and swelling properties of pH-sensitive semi-IPN superabsorbent hydrogels based on sodium alginate-g-poly(sodium acrylate) and polyvinylpyrrolidone. Carbohydrate Polymers, 2010, 80, 1028-1036.	10.2	321
28	Synthesis and characterization of chitosan-g-poly(acrylic acid)/attapulgite superabsorbent composites. Carbohydrate Polymers, 2007, 68, 367-374.	10.2	315
29	Hydrolysis of cellulose into glucose over carbons sulfonated at elevated temperatures. Chemical Communications, 2010, 46, 6935.	4.1	313
30	Removal of methylene blue from aqueous solution using chitosan-g-poly(acrylic) Tj ETQq0 0 0 rgBT /Overlock 10 Engineering Aspects, 2008, 322, 47-53.	Tf 50 307 4.7	' Td (acid)/mc 301
31	Unraveling the coordination structure-performance relationship in Pt1/Fe2O3 single-atom catalyst. Nature Communications, 2019, 10, 4500.	12.8	279
32	Adsorption properties of Congo Red from aqueous solution onto surfactant-modified montmorillonite. Journal of Hazardous Materials, 2008, 160, 173-180.	12.4	274
33	Synthesis of Thermally Stable and Highly Active Bimetallic Auâ^'Ag Nanoparticles on Inert Supports. Chemistry of Materials, 2009, 21, 410-418.	6.7	262
34	Co–N–C Catalyst for C–C Coupling Reactions: On the Catalytic Performance and Active Sites. ACS Catalysis, 2015, 5, 6563-6572.	11.2	260
35	Durable superhydrophobic/superoleophilic PDMS sponges and their applications in selective oil absorption and in plugging oil leakages. Journal of Materials Chemistry A, 2014, 2, 18281-18287.	10.3	259
36	Single-atom catalyst: a rising star for green synthesis of fine chemicals. National Science Review, 2018, 5, 653-672.	9.5	258

#	Article	IF	CITATIONS
37	Synthesis of ethylene glycol and terephthalic acid from biomass for producing PET. Green Chemistry, 2016, 18, 342-359.	9.0	254
38	Superhydrophobic kapok fiber oil-absorbent: Preparation and high oil absorbency. Chemical Engineering Journal, 2012, 213, 1-7.	12.7	253
39	Preparation and characterization of a novel pH-sensitive chitosan-g-poly (acrylic) Tj ETQq1 1 0.784314 rgBT /Over sodium. Carbohydrate Polymers, 2009, 78, 731-737.	lock 10 Tf 10.2	50 667 Td ( 252
40	Studies on poly(acrylic acid)/attapulgite superabsorbent composite. I. Synthesis and characterization. Journal of Applied Polymer Science, 2004, 92, 1596-1603.	2.6	251
41	A new 3D mesoporous carbon replicated from commercial silica as a catalyst support for direct conversion of cellulose into ethylene glycol. Chemical Communications, 2010, 46, 862-864.	4.1	249
42	Fast removal of methylene blue from aqueous solution by adsorption onto chitosan-g-poly (acrylic) Tj ETQq0 0 0 r	gBT/Over	lock 10 Tf 5 244
43	Production of Primary Amines by Reductive Amination of Biomassâ€Derived Aldehydes/Ketones. Angewandte Chemie - International Edition, 2017, 56, 3050-3054.	13.8	243
44	A Durable Nickel Singleâ€Atom Catalyst for Hydrogenation Reactions and Cellulose Valorization under Harsh Conditions. Angewandte Chemie - International Edition, 2018, 57, 7071-7075.	13.8	243
45	Enhanced adsorption of Methylene Blue from aqueous solution by chitosan-g-poly (acrylic) Tj ETQq1 1 0.784314 i	rgBT /Ove 6.1	rlock 10 Tf 5
46	Effect of kapok fiber treated with various solvents on oil absorbency. Industrial Crops and Products, 2012, 40, 178-184.	5.2	231
47	A review on bidirectional analogies between the photocatalysis and antibacterial properties of ZnO. Journal of Alloys and Compounds, 2019, 783, 898-918.	5.5	229
48	Efficient and Durable Au Alloyed Pd Single-Atom Catalyst for the Ullmann Reaction of Aryl Chlorides in Water. ACS Catalysis, 2014, 4, 1546-1553.	11.2	221
49	Dynamic Behavior of Single-Atom Catalysts in Electrocatalysis: Identification of Cu-N <sub>3</sub> as an Active Site for the Oxygen Reduction Reaction. Journal of the American Chemical Society, 2021, 143, 14530-14539.	13.7	218
50	Fast removal of copper ions from aqueous solution by chitosan-g-poly(acrylic acid)/attapulgite composites. Journal of Hazardous Materials, 2009, 168, 970-977.	12.4	216
51	Removal of Cu(II) from aqueous solution by adsorption onto acid-activated palygorskite. Journal of Hazardous Materials, 2007, 149, 346-354.	12.4	215
52	Kinetic and isothermal studies of lead ion adsorption onto palygorskite clay. Journal of Colloid and Interface Science, 2007, 307, 309-316.	9.4	206
53	Zeolite-supported metal catalysts for selective hydrodeoxygenation of biomass-derived platform molecules. Green Chemistry, 2019, 21, 3744-3768.	9.0	200
54	In situ generation of sodium alginate/hydroxyapatite nanocomposite beads as drug-controlled release matrices. Acta Biomaterialia, 2010, 6, 445-454.	8.3	198

#	Article	IF	CITATIONS
55	Strong metal-support interaction promoted scalable production of thermally stable single-atom catalysts. Nature Communications, 2020, 11, 1263.	12.8	198
56	Potential-Driven Restructuring of Cu Single Atoms to Nanoparticles for Boosting the Electrochemical Reduction of Nitrate to Ammonia. Journal of the American Chemical Society, 2022, 144, 12062-12071.	13.7	192
57	Adsorption kinetics of Cu(II) ions using N,O-carboxymethyl-chitosan. Journal of Hazardous Materials, 2006, 131, 103-111.	12.4	190
58	Nanocomposite of carboxymethyl cellulose and attapulgite as a novel pH-sensitive superabsorbent: Synthesis, characterization and properties. Carbohydrate Polymers, 2010, 82, 83-91.	10.2	188
59	Adsorption properties of congo red from aqueous solution onto N,O-carboxymethyl-chitosan. Bioresource Technology, 2008, 99, 1403-1408.	9.6	186
60	Cobalt Single Atoms on Tetrapyridomacrocyclic Support for Efficient Peroxymonosulfate Activation. Environmental Science & Technology, 2021, 55, 1242-1250.	10.0	185
61	Design of a Highly Active Ir/Fe(OH) <sub><i>x</i></sub> Catalyst: Versatile Application of Ptâ€Group Metals for the Preferential Oxidation of Carbon Monoxide. Angewandte Chemie - International Edition, 2012, 51, 2920-2924.	13.8	183
62	Understanding the synergistic effects of gold bimetallic catalysts. Journal of Catalysis, 2013, 308, 258-271.	6.2	178
63	Adsorption of dyes onto palygorskite and its composites: A review. Journal of Environmental Chemical Engineering, 2016, 4, 1274-1294.	6.7	178
64	Synthesis of Highâ€Quality Diesel with Furfural and 2â€Methylfuran from Hemicellulose. ChemSusChem, 2012, 5, 1958-1966.	6.8	177
65	Adsorption characteristics of Cu(II) from aqueous solution onto poly(acrylamide)/attapulgite composite. Journal of Hazardous Materials, 2009, 165, 223-231.	12.4	175
66	UiO-66 derived Ru/ZrO <sub>2</sub> @C as a highly stable catalyst for hydrogenation of levulinic acid to γ-valerolactone. Green Chemistry, 2017, 19, 2201-2211.	9.0	174
67	A simple hydrothermal approach to modify palygorskite for high-efficient adsorption of Methylene blue and Cu(II) ions. Chemical Engineering Journal, 2015, 265, 228-238.	12.7	173
68	Pressure-Sensitive and Conductive Carbon Aerogels from Poplars Catkins for Selective Oil Absorption and Oil/Water Separation. ACS Applied Materials & amp; Interfaces, 2017, 9, 18001-18007.	8.0	173
69	Synthesis and properties of clay-based superabsorbent composite. European Polymer Journal, 2005, 41, 1630-1637.	5.4	172
70	Utilization of starch and clay for the preparation of superabsorbent composite. Bioresource Technology, 2007, 98, 327-332.	9.6	170
71	Synthesis, characterization and swelling behaviors of sodium alginate-g-poly(acrylic acid)/sodium humate superabsorbent. Carbohydrate Polymers, 2009, 75, 79-84.	10.2	169
72	A Schiff base modified gold catalyst for green and efficient H <sub>2</sub> production from formic acid. Energy and Environmental Science, 2015, 8, 3204-3207.	30.8	166

#	Article	IF	CITATIONS
73	Selectivity Control for Cellulose to Diols: Dancing on Eggs. ACS Catalysis, 2017, 7, 1939-1954.	11.2	162

## Adsorption of lead ions from aqueous solution by using carboxymethyl cellulose-g-poly (acrylic) Tj ETQq0 0 0 rgBT $\frac{10}{8.2}$ Tf 50 70

75	<i>Nepenthes</i> Pitcher Inspired Antiâ€Wetting Silicone Nanofilaments Coatings: Preparation, Unique Antiâ€Wetting and Selfâ€Cleaning Behaviors. Advanced Functional Materials, 2014, 24, 1074-1080.	14.9	156
76	Ag nanoparticle-entrapped hydrogel as promising material for catalytic reduction of organic dyes. Journal of Materials Chemistry, 2012, 22, 16552.	6.7	155
77	Adsorption properties of crosslinked carboxymethyl-chitosan resin with Pb(II) as template ions. Journal of Hazardous Materials, 2006, 136, 930-937.	12.4	153
78	Efficient adsorption of methylene blue on an alginate-based nanocomposite hydrogel enhanced by organo-illite/smectite clay. Chemical Engineering Journal, 2013, 228, 132-139.	12.7	153
79	A comparative study about adsorption of natural palygorskite for methylene blue. Chemical Engineering Journal, 2015, 262, 390-398.	12.7	153
80	Adsorption behavior of Cu2+ from aqueous solutions onto starch-g-poly(acrylic acid)/sodium humate hydrogels. Desalination, 2010, 263, 170-175.	8.2	152
81	Temperature-controlled phase-transfer catalysis for ethylene glycol production from cellulose. Chemical Communications, 2012, 48, 7052.	4.1	152
82	Highly selective and robust single-atom catalyst Ru1/NC for reductive amination of aldehydes/ketones. Nature Communications, 2021, 12, 3295.	12.8	152
83	Ordered Crystalline Alumina Molecular Sieves Synthesized via a Nanocasting Route. Chemistry of Materials, 2006, 18, 5153-5155.	6.7	151
84	Catalytic conversion of cellulose to hexitols with mesoporous carbon supported Ni-based bimetallic catalysts. Green Chemistry, 2012, 14, 614.	9.0	151
85	Promotional effect of Pd single atoms on Au nanoparticles supported on silica for the selective hydrogenation of acetylene in excess ethylene. New Journal of Chemistry, 2014, 38, 2043.	2.8	151
86	Maximizing the Number of Interfacial Sites in Singleâ€Atom Catalysts for the Highly Selective, Solventâ€Free Oxidation of Primary Alcohols. Angewandte Chemie - International Edition, 2018, 57, 7795-7799.	13.8	151
87	Adsorption of methylene blue by kapok fiber treated by sodium chlorite optimized with response surface methodology. Chemical Engineering Journal, 2012, 184, 248-255.	12.7	150
88	Evaluation of ammonium removal using a chitosan-g-poly (acrylic acid)/rectorite hydrogel composite. Journal of Hazardous Materials, 2009, 171, 671-677.	12.4	148
89	Facile preparation of durable and robust superhydrophobic textiles by dip coating in nanocomposite solution of organosilanes. Chemical Communications, 2013, 49, 11509.	4.1	147
90	Research and application of kapok fiber as an absorbing material: A mini review. Journal of Environmental Sciences, 2015, 27, 21-32.	6.1	147

#	Article	IF	CITATIONS
91	One-pot fabrication of multifunctional superparamagnetic attapulgite/Fe <sub>3</sub> O <sub>4</sub> /polyaniline nanocomposites served as an adsorbent and catalyst support. Journal of Materials Chemistry A, 2015, 3, 281-289.	10.3	146
92	Synthesis of renewable high-density fuels using cyclopentanone derived from lignocellulose. Chemical Communications, 2014, 50, 2572.	4.1	143
93	Cerium-Oxide-Modified Nickel as a Non-Noble Metal Catalyst for Selective Decomposition of Hydrous Hydrazine to Hydrogen. ACS Catalysis, 2015, 5, 1623-1628.	11.2	143
94	Ultralight, compressible and multifunctional carbon aerogels based on natural tubular cellulose. Journal of Materials Chemistry A, 2016, 4, 2069-2074.	10.3	141
95	Valorization of Lignin to Simple Phenolic Compounds over Tungsten Carbide: Impact of Lignin Structure. ChemSusChem, 2017, 10, 523-532.	6.8	141
96	Hydrogenolysis of Glycerol to 1,3â€propanediol under Low Hydrogen Pressure over WO <sub><i>x</i></sub> ‣upported Single/Pseudo‣ingle Atom Pt Catalyst. ChemSusChem, 2016, 9, 784-790.	6.8	140
97	Preparation and Properties of Chitosan-g-poly(acrylic acid)/Montmorillonite Superabsorbent Nanocomposite via in Situ Intercalative Polymerization. Industrial & Engineering Chemistry Research, 2007, 46, 2497-2502.	3.7	139
98	Preparation and swelling properties of pH-sensitive composite hydrogel beads based on chitosan-g-poly (acrylic acid)/vermiculite and sodium alginate for diclofenac controlled release. International Journal of Biological Macromolecules, 2010, 46, 356-362.	7.5	138
99	Aqueous phase hydrogenation of levulinic acid to 1,4-pentanediol. Chemical Communications, 2014, 50, 1414.	4.1	136
100	Study on superabsorbent composites. IX: Synthesis, characterization and swelling behaviors of polyacrylamide/clay composites based on various clays. Reactive and Functional Polymers, 2007, 67, 737-745.	4.1	134
101	Green Synthesis and Characterization of Anisotropic Uniform Single-Crystal α-MoO3Nanostructures. Journal of Physical Chemistry C, 2007, 111, 2401-2408.	3.1	133
102	Attapulgite/bentonite interactions for methylene blue adsorption characteristics from aqueous solution. Chemical Engineering Journal, 2014, 237, 403-410.	12.7	133
103	One-step in situ fabrication of a granular semi-IPN hydrogel based on chitosan and gelatin for fast and efficient adsorption of Cu2+ ion. Colloids and Surfaces B: Biointerfaces, 2013, 106, 51-59.	5.0	132
104	Catalytic Conversion of Cellulose to Ethylene Glycol over a Low ost Binary Catalyst of Raney Ni and Tungstic Acid. ChemSusChem, 2013, 6, 652-658.	6.8	132
105	Recent progress in dispersion of palygorskite crystal bundles for nanocomposites. Applied Clay Science, 2016, 119, 18-30.	5.2	130
106	A novel pH sensitive <i>N</i> â€succinyl chitosan/alginate hydrogel bead for nifedipine delivery. Biopharmaceutics and Drug Disposition, 2008, 29, 173-184.	1.9	128
107	Catalytically Active Rh Subâ€Nanoclusters on TiO <sub>2</sub> for CO Oxidation at Cryogenic Temperatures. Angewandte Chemie - International Edition, 2016, 55, 2820-2824.	13.8	127
108	Synthesis of 1,6-hexanediol from HMF over double-layered catalysts of Pd/SiO <sub>2</sub> + Ir–ReO <sub>x</sub> /SiO <sub>2</sub> in a fixed-bed reactor. Green Chemistry, 2016, 18, 2175-2184.	9.0	127

#	Article	IF	CITATIONS
109	ZnAlâ€Hydrotalcite‣upported Au <sub>25</sub> Nanoclusters as Precatalysts for Chemoselective Hydrogenation of 3â€Nitrostyrene. Angewandte Chemie - International Edition, 2017, 56, 2709-2713.	13.8	127
110	Cooperative Pollutant Adsorption and Persulfate-Driven Oxidation on Hierarchically Ordered Porous Carbon. Environmental Science & Technology, 2019, 53, 10352-10360.	10.0	127
111	Glycol assisted synthesis of graphene–MnO2–polyaniline ternary composites for high performance supercapacitor electrodes. Physical Chemistry Chemical Physics, 2014, 16, 7872.	2.8	126
112	Study on superabsorbent composite XVI. Synthesis, characterization and swelling behaviors of poly(sodium acrylate)/vermiculite superabsorbent composites. European Polymer Journal, 2007, 43, 1691-1698.	5.4	124
113	Singleâ€Atom Catalysis in Mesoporous Photovoltaics: The Principle of Utility Maximization. Advanced Materials, 2014, 26, 8147-8153.	21.0	122
114	Effect of Various Dissolution Systems on the Molecular Weight of Regenerated Silk Fibroin. Biomacromolecules, 2013, 14, 285-289.	5.4	120
115	Catalytic Hydrogenation of Corn Stalk to Ethylene Glycol and 1,2-Propylene Glycol. Industrial & Engineering Chemistry Research, 2011, 50, 6601-6608.	3.7	119
116	One-Step Synthesis of Au–Pd Alloy Nanodendrites and Their Catalytic Activity. Journal of Physical Chemistry C, 2013, 117, 12526-12536.	3.1	119
117	Synthesis of renewable diesel with hydroxyacetone and 2-methyl-furan. Chemical Communications, 2013, 49, 5727.	4.1	116
118	Structural and catalytic properties of supported Ni–Ir alloy catalysts for H2 generation via hydrous hydrazine decomposition. Applied Catalysis B: Environmental, 2014, 147, 779-788.	20.2	116
119	Adsorption behaviors of Congo red on the N,O-carboxymethyl-chitosan/montmorillonite nanocomposite. Chemical Engineering Journal, 2008, 143, 43-50.	12.7	115
120	Kapok fiber oriented-polyaniline nanofibers for efficient Cr(VI) removal. Chemical Engineering Journal, 2012, 191, 154-161.	12.7	115
121	Preparation, characterization and properties of superabsorbent nanocomposites based on natural guar gum and modified rectorite. Carbohydrate Polymers, 2009, 77, 891-897.	10.2	114
122	Aerobic oxidative coupling of alcohols and amines over Au–Pd/resin in water: Au/Pd molar ratios switch the reaction pathways to amides or imines. Green Chemistry, 2013, 15, 2680.	9.0	114
123	Coated kapok fiber for removal of spilled oil. Marine Pollution Bulletin, 2013, 69, 91-96.	5.0	114
124	Controlling CO <sub>2</sub> Hydrogenation Selectivity by Metal‣upported Electron Transfer. Angewandte Chemie - International Edition, 2020, 59, 19983-19989.	13.8	114
125	Integrated Conversion of Cellulose to High-Density Aviation Fuel. Joule, 2019, 3, 1028-1036.	24.0	113
126	Dual-heteroatom-modified ordered mesoporous carbon: Hydrothermal functionalization, structure, and its electrochemical performance. Journal of Materials Chemistry, 2012, 22, 4963.	6.7	110

#	Article	IF	CITATIONS
127	Alkali activation of halloysite for adsorption and release of ofloxacin. Applied Surface Science, 2013, 287, 54-61.	6.1	110
128	Removal of Methyl Violet from aqueous solutions using poly (acrylic acid-co-acrylamide)/attapulgite composite. Journal of Environmental Sciences, 2010, 22, 7-14.	6.1	109
129	Superwetting Double-Layer Polyester Materials for Effective Removal of Both Insoluble Oils and Soluble Dyes in Water. ACS Applied Materials & Interfaces, 2014, 6, 11581-11588.	8.0	109
130	In-situ synthesis of single-atom Ir by utilizing metal-organic frameworks: An acid-resistant catalyst for hydrogenation of levulinic acid to γ-valerolactone. Journal of Catalysis, 2019, 373, 161-172.	6.2	109
131	Synthesis and characterization of chitosan-g-poly(acrylic acid)/sodium humate superabsorbent. Carbohydrate Polymers, 2007, 70, 166-173.	10.2	107
132	Biomass into chemicals: One-pot production of furan-based diols from carbohydrates via tandem reactions. Catalysis Today, 2014, 234, 59-65.	4.4	107
133	Adsorption characteristics of Cd(II) from aqueous solution onto activated palygorskite. Separation and Purification Technology, 2007, 55, 157-164.	7.9	106
134	Swelling characteristics and drug delivery properties of nifedipineâ€loaded pH sensitive alginate–chitosan hydrogel beads. Journal of Biomedical Materials Research - Part B Applied Biomaterials, 2008, 86B, 493-500.	3.4	106
135	Controlled release of ofloxacin from chitosan–montmorillonite hydrogel. Applied Clay Science, 2010, 50, 112-117.	5.2	104
136	Chitosan-g-poly(acrylic acid) hydrogel with crosslinked polymeric networks for Ni2+ recovery. Analytica Chimica Acta, 2011, 687, 193-200.	5.4	104
137	Synthesis of Diesel or Jet Fuel Range Cycloalkanes with 2-Methylfuran and Cyclopentanone from Lignocellulose. Energy & Fuels, 2014, 28, 5112-5118.	5.1	104
138	Study on superabsorbent composite. VI. Preparation, characterization and swelling behaviors of starch phosphate-graft-acrylamide/attapulgite superabsorbent composite. Carbohydrate Polymers, 2006, 65, 150-158.	10.2	103
139	Adsorption properties of carboxymethyl-chitosan and cross-linked carboxymethyl-chitosan resin with Cu(II) as template. Separation and Purification Technology, 2006, 49, 197-204.	7.9	103
140	Catalytic Conversion of Concentrated Glucose to Ethylene Glycol with Semicontinuous Reaction System. Industrial & Engineering Chemistry Research, 2013, 52, 9566-9572.	3.7	103
141	Highâ€Đensity and Thermally Stable Palladium Singleâ€Atom Catalysts for Chemoselective Hydrogenations. Angewandte Chemie - International Edition, 2020, 59, 21613-21619.	13.8	103
142	Study on superabsorbent composite. III. Swelling behaviors of polyacrylamide/attapulgite composite based on acidified attapulgite and organo-attapulgite. European Polymer Journal, 2005, 41, 2434-2442.	5.4	102
143	Effect of dry grinding on the microstructure of palygorskite and adsorption efficiency for methylene blue. Powder Technology, 2012, 225, 124-129.	4.2	100
144	In situ generation of sodium alginate/hydroxyapatite/halloysite nanotubes nanocomposite hydrogel beads as drug-controlled release matrices. Journal of Materials Chemistry B, 2013, 1, 6261.	5.8	100

#	Article	IF	CITATIONS
145	Fast removal of ammonium ion using a hydrogel optimized with response surface methodology. Chemical Engineering Journal, 2011, 171, 1201-1208.	12.7	98
146	Mechanical- and oil-durable superhydrophobic polyester materials for selective oil absorption and oil/water separation. Journal of Colloid and Interface Science, 2014, 413, 112-117.	9.4	98
147	Synthesis of diesel and jet fuel range alkanes with furfural and ketones from lignocellulose under solvent free conditions. Green Chemistry, 2014, 16, 4879-4884.	9.0	97
148	Removal of heavy metals using polyvinyl alcohol semi-IPN poly(acrylic acid)/tourmaline composite optimized with response surface methodology. Chemical Engineering Journal, 2010, 162, 186-193.	12.7	96
149	Surfactant effects on the microstructures of Fe3O4 nanoparticles synthesized by microemulsion method. Colloids and Surfaces A: Physicochemical and Engineering Aspects, 2013, 436, 675-683.	4.7	96
150	Ferric Oxide-Supported Pt Subnano Clusters for Preferential Oxidation of CO in H <sub>2</sub> -Rich Gas at Room Temperature. ACS Catalysis, 2014, 4, 2113-2117.	11.2	96
151	Highly active Au1/Co3O4 single-atom catalyst for CO oxidation at room temperature. Chinese Journal of Catalysis, 2015, 36, 1505-1511.	14.0	93
152	Versatile Nickel–Lanthanum(III) Catalyst for Direct Conversion of Cellulose to Glycols. ACS Catalysis, 2015, 5, 874-883.	11.2	92
153	Mimic nature, beyond nature: facile synthesis of durable superhydrophobic textiles using organosilanes. Journal of Materials Chemistry B, 2013, 1, 4756.	5.8	91
154	Hydrodeoxygenation of furans over Pd-FeOx/SiO2 catalyst under atmospheric pressure. Applied Catalysis B: Environmental, 2017, 201, 266-277.	20.2	91
155	Preparation of starch-graft-poly(acrylamide)/attapulgite superabsorbent composite. Journal of Applied Polymer Science, 2005, 98, 1351-1357.	2.6	90
156	Magnetically driven super durable superhydrophobic polyester materials for oil/water separation. Polymer Chemistry, 2014, 5, 2382.	3.9	90
157	Current fundamental and applied research into clay minerals in China. Applied Clay Science, 2016, 119, 3-7.	5.2	90
158	Remarkable effect of alkalis on the chemoselective hydrogenation of functionalized nitroarenes over high-loading Pt/FeO <sub>x</sub> catalysts. Chemical Science, 2017, 8, 5126-5131.	7.4	90
159	Selective Hydrogenolysis of Glycerol to 1,3â€Propanediol: Manipulating the Frustrated Lewis Pairs by Introducing Gold to Pt/WO <sub><i>x</i></sub> . ChemSusChem, 2017, 10, 819-824.	6.8	89
160	Fast removal of ammonium nitrogen from aqueous solution using chitosan-g-poly(acrylic) Tj ETQq0 0 0 rgBT /Ove	erlock 10 7 12.7	Tf 50 142 Td
	Synthesis of renewable diesel with the 2-methylfuran, butanal and acetone derived from		

161	lignocellulose. Bioresource Technology, 2013, 134, 66-72.	9.6	88
162	Mussel and fish scale-inspired underwater superoleophobic kapok membranes for continuous and simultaneous removal of insoluble oils and soluble dyes in water. Journal of Materials Chemistry A, 2015, 3, 18475-18482.	10.3	88

#	Article	IF	CITATIONS
163	Colorful Superamphiphobic Coatings with Low Sliding Angles and High Durability Based on Natural Nanorods. ACS Applied Materials & Interfaces, 2017, 9, 1941-1952.	8.0	88
164	Studies on poly(acrylic acid)/attapulgite superabsorbent composites. II. Swelling behaviors of superabsorbent composites in saline solutions and hydrophilic solvent-water mixtures. Journal of Applied Polymer Science, 2004, 94, 1869-1876.	2.6	86
165	Adsorption and release of ofloxacin from acid- and heat-treated halloysite. Colloids and Surfaces B: Biointerfaces, 2014, 113, 51-58.	5.0	86
166	Investigation of acetylated kapok fibers on the sorption of oil in water. Journal of Environmental Sciences, 2013, 25, 246-253.	6.1	85
167	Single atom gold catalysts for low-temperature CO oxidation. Chinese Journal of Catalysis, 2016, 37, 1580-1586.	14.0	85
168	Synthesis of Diesel and Jet Fuel Range Alkanes with Furfural and Angelica Lactone. ACS Catalysis, 2017, 7, 5880-5886.	11.2	85
169	Highly efficient and selective adsorption of malachite green onto granular composite hydrogel. Chemical Engineering Journal, 2014, 257, 66-73.	12.7	84
170	Monolithic supermacroporous hydrogel prepared from high internal phase emulsions (HIPEs) for fast removal of Cu 2+ and Pb 2+. Chemical Engineering Journal, 2016, 284, 422-430.	12.7	84
171	Selectivity-Switchable Conversion of Cellulose to Glycols over Ni–Sn Catalysts. ACS Catalysis, 2016, 6, 191-201.	11.2	83
172	Evaporation-Induced Transition from <i>Nepenthes</i> Pitcher-Inspired Slippery Surfaces to Lotus Leaf-Inspired Superoleophobic Surfaces. Langmuir, 2014, 30, 14292-14299.	3.5	82
173	Facile and green fabrication of magnetically recyclable carboxyl-functionalized attapulgite/carbon nanocomposites derived from spent bleaching earth for wastewater treatment. Chemical Engineering Journal, 2017, 322, 102-114.	12.7	81
174	Bioinspired copper singleâ€atom nanozyme as a superoxide dismutaseâ€like antioxidant for sepsis treatment. Exploration, 2022, 2, .	11.0	81
175	Synthesis, swelling and responsive properties of a new composite hydrogel based on hydroxyethyl cellulose and medicinal stone. Composites Part B: Engineering, 2011, 42, 809-818.	12.0	80
176	Investigation of Rheological Properties and Conformation of Silk Fibroin in the Solution of AmimCl. Biomacromolecules, 2012, 13, 1875-1881.	5.4	80
177	One-step fabrication in aqueous solution of a granular alginate-based hydrogel for fast and efficient removal of heavy metal ions. Journal of Polymer Research, 2013, 20, 1.	2.4	80
178	Synthesis of renewable diesel range alkanes by hydrodeoxygenation of furans over Ni/Hβ under mild conditions. Green Chemistry, 2014, 16, 594-599.	9.0	79
179	Theoretical investigations of non-noble metal single-atom catalysis: Ni <sub>1</sub> /FeO <sub>x</sub> for CO oxidation. Catalysis Science and Technology, 2016, 6, 6886-6892.	4.1	79
180	A sustainable approach to fabricate new 1D and 2D nanomaterials from natural abundant palygorskite clay for antibacterial and adsorption. Chemical Engineering Journal, 2020, 382, 122984.	12.7	79

#	Article	IF	CITATIONS
181	Making JPâ€10 Superfuel Affordable with a Lignocellulosic Platform Compound. Angewandte Chemie - International Edition, 2019, 58, 12154-12158.	13.8	78
182	Preparation of porous adsorbent via Pickering emulsion template for water treatment: A review. Journal of Environmental Sciences, 2020, 88, 217-236.	6.1	78
183	Phosphorus coordinated Rh single-atom sites on nanodiamond as highly regioselective catalyst for hydroformylation of olefins. Nature Communications, 2021, 12, 4698.	12.8	78
184	Adsorption of Pb(II) from Aqueous Solution by Chitosan- <i>g</i> -poly(acrylic acid)/Attapulgite/Sodium Humate Composite Hydrogels. Journal of Chemical & Engineering Data, 2010, 55, 2379-2384.	1.9	77
185	Investigation of oil sorption capability of PBMA/SiO2 coated kapok fiber. Chemical Engineering Journal, 2013, 223, 632-637.	12.7	77
186	Synthesis of covalently crosslinked attapulgite/poly(acrylic acid-co-acrylamide) nanocomposite hydrogels and their evaluation as adsorbent for heavy metal ions. Journal of Industrial and Engineering Chemistry, 2015, 23, 188-193.	5.8	77
187	Hydrogenolysis of methyl glycolate to ethanol over a Pt–Cu/SiO <sub>2</sub> single-atom alloy catalyst: a further step from cellulose to ethanol. Green Chemistry, 2018, 20, 2142-2150.	9.0	77
188	Selective aldol condensation of biomass-derived levulinic acid and furfural in aqueous-phase over MgO and ZnO. Green Chemistry, 2016, 18, 3430-3438.	9.0	76
189	Adsorption properties and mechanism of cross-linked carboxymethyl-chitosan resin with Zn(II) as template ion. Reactive and Functional Polymers, 2006, 66, 819-826.	4.1	75
190	Mechanical and water resistance properties of chitosan/poly(vinyl alcohol) films reinforced with attapulgite dispersed by high-pressure homogenization. Chemical Engineering Journal, 2012, 210, 166-172.	12.7	75
191	Photo–thermo Catalytic Oxidation over a TiO <sub>2</sub> â€WO <sub>3</sub> ‣upported Platinum Catalyst. Angewandte Chemie - International Edition, 2020, 59, 12909-12916.	13.8	75
192	pH-responsive carboxymethylcellulose-g-poly(sodium acrylate)/polyvinylpyrrolidone semi-IPN hydrogels with enhanced responsive and swelling properties. Macromolecular Research, 2011, 19, 57-65.	2.4	74
193	Selective Production of 1,2â€Propylene Glycol from Jerusalem Artichoke Tuber using Ni–W <sub>2</sub> C/AC Catalysts. ChemSusChem, 2012, 5, 932-938.	6.8	74
194	Kinetic study of retroâ€aldol condensation of glucose to glycolaldehyde with ammonium metatungstate as the catalyst. AICHE Journal, 2014, 60, 3804-3813.	3.6	74
195	From Maya blue to biomimetic pigments: durable biomimetic pigments with self-cleaning property. Journal of Materials Chemistry A, 2016, 4, 901-907.	10.3	74
196	A functionalized hybrid silicate adsorbent derived from naturally abundant low-grade palygorskite clay for highly efficient removal of hazardous antibiotics. Chemical Engineering Journal, 2016, 293, 376-385.	12.7	74
197	Mild Redox-Neutral Depolymerization of Lignin with a Binuclear Rh Complex in Water. ACS Catalysis, 2019, 9, 4441-4447.	11.2	74
198	Styrene Hydroformylation with In Situ Hydrogen: Regioselectivity Control by Coupling with the Lowâ€Temperature Water–Gas Shift Reaction. Angewandte Chemie - International Edition, 2020, 59, 7430-7434.	13.8	74

#	Article	IF	CITATIONS
199	Study on superabsorbent composite. V. Synthesis, swelling behaviors and application of poly(acrylic) Tj ETQq1 1 Technologies, 2005, 16, 813-820.	0.784314 3.2	rgBT /Over 73
200	Rapid and wide pH-independent ammonium-nitrogen removal using a composite hydrogel with three-dimensional networks. Chemical Engineering Journal, 2012, 179, 90-98.	12.7	73
201	One-Step Calcination of the Spent Bleaching Earth for the Efficient Removal of Heavy Metal Ions. ACS Sustainable Chemistry and Engineering, 2015, 3, 1125-1135.	6.7	73
202	Lignosulfonate-based acidic resin for the synthesis of renewable diesel and jet fuel range alkanes with 2-methylfuran and furfural. Green Chemistry, 2015, 17, 3644-3652.	9.0	73
203	Chemocatalytic Conversion of Cellulosic Biomass to Methyl Glycolate, Ethylene Glycol, and Ethanol. ChemSusChem, 2017, 10, 1390-1394.	6.8	73
204	One-Pot Production of Cellulosic Ethanol via Tandem Catalysis over a Multifunctional Mo/Pt/WOx Catalyst. Joule, 2019, 3, 1937-1948.	24.0	73
205	Highly Selective Oxidation of Methane into Methanol over Cu-Promoted Monomeric Fe/ZSM-5. ACS Catalysis, 2021, 11, 6684-6691.	11.2	73
206	One-pot catalytic conversion of cellulose to ethylene glycol and other chemicals: From fundamental discovery to potential commercialization. Chinese Journal of Catalysis, 2014, 35, 602-613.	14.0	72
207	Tungsten Carbide: A Remarkably Efficient Catalyst for the Selective Cleavage of Lignin Câ^'O Bonds. ChemSusChem, 2016, 9, 3220-3229.	6.8	72
208	Synthesis and characterization of multifunctional poly(acrylic acid-co-acrylamide)/sodium humate superabsorbent composite. Reactive and Functional Polymers, 2006, 66, 747-756.	4.1	71
209	Effect of surfactant on porosity and swelling behaviors of guar gum-g-poly(sodium) Tj ETQq1 1 0.784314 rgBT / 2011, 88, 279-286.	Overlock 1 5.0	0 Tf 50 347 71
210	Catalytic cascade conversion of furfural to 1,4-pentanediol in a single reactor. Green Chemistry, 2018, 20, 1770-1776.	9.0	71
211	Facile preparation of super durable superhydrophobic materials. Journal of Colloid and Interface Science, 2014, 432, 31-42.	9.4	70
212	Superadsorbent with three-dimensional networks: From bulk hydrogel to granular hydrogel. European Polymer Journal, 2015, 72, 661-686.	5.4	69
213	A simple approach to fabricate granular adsorbent for adsorption of rare elements. International Journal of Biological Macromolecules, 2015, 72, 410-420.	7.5	69
214	Single-atom Pt promoted Mo2C for electrochemical hydrogen evolution reaction. Journal of Energy Chemistry, 2021, 57, 371-377.	12.9	69
215	Adsorption properties of N-succinyl-chitosan and cross-linked N-succinyl-chitosan resin with Pb(II) as template ions. Separation and Purification Technology, 2006, 51, 409-415.	7.9	67
216	Hydroformylation of Olefins by a Rhodium Singleâ€Atom Catalyst with Activity Comparable to RhCl(PPh <sub>3</sub> ) <sub>3</sub> . Angewandte Chemie, 2016, 128, 16288-16292.	2.0	67

#	Article	IF	CITATIONS
21'	Durable Superhydrophobic/Superoleophilic Polyurethane Sponges Inspired by Mussel and Lotus Leaf for the Selective Removal of Organic Pollutants from Water. ChemPlusChem, 2014, 79, 850-856.	2.8	66
21	Facile fabrication of superparamagnetic graphene/polyaniline/Fe3O4 nanocomposites for fast magnetic separation and efficient removal of dye. Scientific Reports, 2017, 7, 5347.	3.3	66
21	<ul> <li>Effective Hydrogenolysis of Glycerol to 1,3â€Propanediol over Metalâ€Acid Concerted</li> <li>Pt/WO<sub>x</sub>/Al<sub>2</sub>O<sub>3</sub> Catalysts. ChemCatChem, 2019, 11, 3903-3912.</li> </ul>	3.7	66
22	Enhanced Adsorption of Ammonium Using Hydrogel Composites Based on Chitosan and Halloysite. Journal of Macromolecular Science - Pure and Applied Chemistry, 2009, 47, 33-38.	2.2	65
22	Kapok Fiber Oriented Polyaniline for Removal of Sulfonated Dyes. Industrial & amp; Engineering Chemistry Research, 2012, 51, 10079-10087.	3.7	65
22	Removal of methylene blue from aqueous solution by sorption on lignocellulose-g-poly(acrylic) Tj ETQqO O O Bulletin, 2013, 70, 1163-1179.	rgBT /Overlock 3.3	10 Tf 50 54 64
22	Rapid enrichment of rare-earth metals by carboxymethyl cellulose-based open-cellular hydrogel adsorbent from HIPEs template. Carbohydrate Polymers, 2016, 140, 51-58.	10.2	64
22	<ul> <li>Production of Primary Amines by Reductive Amination of Biomassâ€Derived Aldehydes/Ketones.</li> <li>Angewandte Chemie, 2017, 129, 3096-3100.</li> </ul>	2.0	64
22	A Durable Nickel Singleâ€Atom Catalyst for Hydrogenation Reactions and Cellulose Valorization under Harsh Conditions. Angewandte Chemie, 2018, 130, 7189-7193.	2.0	64
22	Study on superabsorbent composites XIX. Synthesis, characterization and performance of chitosan-g-poly (acrylic acid)/vermiculite superabsorbent composites. Journal of Polymer Research, 2009, 16, 143-150.	2.4	63
22	7 Mesoporous Ti–W oxide: synthesis, characterization, and performance in selective hydrogenolysis of glycerol. Journal of Materials Chemistry A, 2013, 1, 3724.	10.3	63
22	<ul> <li>Surface Oxygen Vacancy-Dependent Electrocatalytic Activity of W<sub>18</sub>O<sub>49</sub></li> <li>Nanowires. Journal of Physical Chemistry C, 2014, 118, 20100-20106.</li> </ul>	3.1	62
22	Robustly superhydrophobic/superoleophilic kapok fiber with ZnO nanoneedles coating: Highly efficient separation of oil layer in water and capture of oil droplets in oil-in-water emulsions. Industrial Crops and Products, 2017, 108, 303-311.	5.2	62
23	O Unlock the Compact Structure of Lignocellulosic Biomass by Mild Ball Milling for Ethylene Glycol Production. ACS Sustainable Chemistry and Engineering, 2019, 7, 679-687.	6.7	62
23	Disaggregation of palygorskite crystal bundles via high-pressure homogenization. Applied Clay Science, 2011, 54, 118-123.	5.2	61
23	<ul> <li>Highly effective removal of Methylene Blue using functionalized attapulgite via hydrothermal</li> <li>process. Journal of Environmental Sciences, 2015, 33, 106-115.</li> </ul>	6.1	61
23	<ul> <li>Preparation of granular hydrogel composite by the redox couple for efficient and fast adsorption of</li> <li>La(III) and Ce(III). Journal of Environmental Chemical Engineering, 2015, 3, 1416-1425.</li> </ul>	6.7	61
23	Removal of Organic Pollutants from Water Using Superwetting Materials. Chemical Record, 2018, 18, 118-136.	5.8	61

#	Article	IF	CITATIONS
235	Synthesis of gasoline and jet fuel range cycloalkanes and aromatics from poly(ethylene terephthalate) waste. Green Chemistry, 2019, 21, 2709-2719.	9.0	61
236	Synthesis of high density aviation fuel with cyclopentanol derived from lignocellulose. Scientific Reports, 2015, 5, 9565.	3.3	60
237	Facile fabrication of well-defined microtubular carbonized kapok fiber/NiO composites as electrode material for supercapacitor. Electrochimica Acta, 2016, 194, 84-94.	5.2	60
238	Synthesis of Renewable High-Density Fuel with Cyclopentanone Derived from Hemicellulose. ACS Sustainable Chemistry and Engineering, 2017, 5, 1812-1817.	6.7	60
239	Antimicrobial Activity of Zinc Oxide–Graphene Quantum Dot Nanocomposites: Enhanced Adsorption on Bacterial Cells by Cationic Capping Polymers. ACS Sustainable Chemistry and Engineering, 2019, 7, 16264-16273.	6.7	59
240	Mesoporous WO3 Supported Pt Catalyst for Hydrogenolysis of Glycerol to 1,3-Propanediol. Chinese Journal of Catalysis, 2012, 33, 1257-1261.	14.0	58
241	Effects of synbiotic supplementation on growth performance, carcass characteristics, meat quality and muscular antioxidant capacity and mineral contents in broilers. Journal of the Science of Food and Agriculture, 2017, 97, 3699-3705.	3.5	58
242	Novel approach for attapulgite/poly(acrylic acid) (ATP/PAA) nanocomposite microgels as selective adsorbent for Pb(II) Ion. Reactive and Functional Polymers, 2014, 74, 72-80.	4.1	57
243	Bright blue halloysite/CoAl 2 O 4 hybrid pigments: Preparation, characterization and application in water-based painting. Dyes and Pigments, 2017, 139, 473-481.	3.7	57
244	Natural cellulose fiber derived hollow-tubular-oriented polydopamine: In-situ formation of Ag nanoparticles for reduction of 4-nitrophenol. Carbohydrate Polymers, 2017, 158, 44-50.	10.2	57
245	Novel environment friendly inorganic red pigments based on attapulgite. Powder Technology, 2017, 315, 60-67.	4.2	56
246	One-step synthesis of magnetic attapulgite/carbon supported NiFe-LDHs by hydrothermal process of spent bleaching earth for pollutants removal. Journal of Cleaner Production, 2018, 172, 673-685.	9.3	56
247	Synthesis, characterization and water absorbency properties of poly(acrylic acid)/sodium humate superabsorbent composite. Polymers for Advanced Technologies, 2005, 16, 675-680.	3.2	55
248	Preparation, Swelling Behaviors, and Slow-Release Properties of a Poly(acrylic) Tj ETQq0 0 0 rgBT /Overlock 10 Tf Research, 2006, 45, 48-53.	50 227 Tc 3.7	l (acid-co-acry 55
249	Synthesis of Jet-Fuel Range Cycloalkanes from the Mixtures of Cyclopentanone and Butanal. Industrial & Engineering Chemistry Research, 2015, 54, 11825-11837.	3.7	55
250	Protonated titanate nanotubes as a highly active catalyst for the synthesis of renewable diesel and jet fuel range alkanes. Applied Catalysis B: Environmental, 2015, 170-171, 124-134.	20.2	55
251	Potential of Calotropis gigantea fiber as an absorbent for removal of oil from water. Industrial Crops and Products, 2016, 83, 387-390.	5.2	55
252	In situ encapsulation of iron(0) for solar thermochemical syngas production over iron-based perovskite material. Communications Chemistry, 2018, 1, .	4.5	55

#	Article	IF	CITATIONS
253	Removal of Congo red from aqueous solution using a chitosan/organo―montmorillonite nanocomposite. Journal of Chemical Technology and Biotechnology, 2007, 82, 711-720.	3.2	54
254	Syntheses and properties of superabsorbent composites based on natural guar gum and attapulgite. Polymers for Advanced Technologies, 2008, 19, 1852-1859.	3.2	54
255	Perfluorosilane treated Calotropis gigantea fiber: Instant hydrophobic–oleophilic surface with efficient oil-absorbing performance. Chemical Engineering Journal, 2016, 295, 477-483.	12.7	54
256	Direct Catalytic Hydrogenolysis of Kraft Lignin to Phenols in Choline-Derived Ionic Liquids. ACS Sustainable Chemistry and Engineering, 2016, 4, 3850-3856.	6.7	54
257	Synthesis, swelling behaviors, and slowâ€release characteristics of a guar gumâ€ <i>g</i> â€poly(sodium) Tj ETQq2	1 <u>1 0</u> .7843 2.6	314 rgBT /
258	A novel pH-sensitive magnetic alginate–chitosan beads for albendazole delivery. Drug Development and Industrial Pharmacy, 2010, 36, 867-877.	2.0	53
259	Synthesis, characterization, and swelling behaviors of chitosanâ€∢i>gâ€poly(acrylic acid)/poly(vinyl) Tj ETQq1	1,0,7843 3 <b>.</b> 2	14 rgBT /C
260	Preparation of a polyelectrolyte-coated magnetic attapulgite composite for the adsorption of precious metals. Journal of Materials Chemistry A, 2013, 1, 4804.	10.3	53
261	Catalytic conversion of concentrated miscanthus in water for ethylene glycol production. AICHE Journal, 2014, 60, 2254-2262.	3.6	53
262	Oxygen surface groups of activated carbon steer the chemoselective hydrogenation of substituted nitroarenes over nickel nanoparticles. Chemical Communications, 2017, 53, 1969-1972.	4.1	53
263	Tuning the coordination environment of single-atom catalyst M-N-C towards selective hydrogenation of functionalized nitroarenes. Nano Research, 2022, 15, 519-527.	10.4	53
264	Preparation and swelling properties of superabsorbent nanocomposites based on natural guar gum and organo-vermiculite. Applied Clay Science, 2009, 46, 21-26.	5.2	52
265	Preparation, Characterization, and Drug-Release Behaviors of a pH-Sensitive Composite Hydrogel Bead Based on Guar Gum, Attapulgite, and Sodium Alginate. International Journal of Polymeric Materials and Polymeric Biomaterials, 2013, 62, 369-376.	3.4	52
266	Tungstenâ€Based Bimetallic Catalysts for Selective Cleavage of Lignin Câ^'O Bonds. ChemCatChem, 2018, 10, 415-421.	3.7	52
267	Fabrication of magnetic macroporous chitosan- g -poly (acrylic acid) hydrogel for removal of Cd 2+ and Pb 2+. International Journal of Biological Macromolecules, 2016, 93, 483-492.	7.5	51
268	Response Surface Methodology for Optimizing Adsorption Process Parameters for Methylene Blue Removal by a Hydrogel Composite. Adsorption Science and Technology, 2010, 28, 913-922.	3.2	50
269	Synthesis of High-Density Aviation Fuel with Cyclopentanol. ACS Sustainable Chemistry and Engineering, 2016, 4, 6160-6166.	6.7	50
270	Fast and high-capacity adsorption of Rb + and Cs + onto recyclable magnetic porous spheres. Chemical Engineering Journal, 2017, 327, 982-991.	12.7	50

#	Article	IF	CITATIONS
271	On the mechanism of H2 activation over single-atom catalyst: An understanding of Pt1/WO in the hydrogenolysis reaction. Chinese Journal of Catalysis, 2020, 41, 524-532.	14.0	50
272	Study on superabsorbent composite. IV. Effects of organification degree of attapulgite on swelling behaviors of polyacrylamide/organo-attapulgite composites. European Polymer Journal, 2006, 42, 101-108.	5.4	49
273	Kinetic study of the competitive hydrogenation of glycolaldehyde and glucose on Ru/C with or without AMT. AICHE Journal, 2015, 61, 224-238.	3.6	49
274	Nanoscale dispersion crystal bundles of palygorskite by associated modification with phytic acid and high-pressure homogenization for enhanced colloidal properties. Powder Technology, 2015, 269, 85-92.	4.2	49
275	Fabrication of magnetic hydroxypropyl cellulose-g-poly(acrylic acid) porous spheres via Pickering high internal phase emulsion for removal of Cu2+ and Cd2+. Carbohydrate Polymers, 2016, 149, 242-250.	10.2	49
276	Magnetic chitosan–based adsorbent prepared via Pickering high internal phase emulsion for high-efficient removal of antibiotics. International Journal of Biological Macromolecules, 2018, 106, 870-877.	7.5	49
277	Selective conversion of concentrated glucose to 1,2-propylene glycol and ethylene glycol by using RuSn/AC catalysts. Applied Catalysis B: Environmental, 2018, 239, 300-308.	20.2	49
278	A new route to fabricate high-efficient porous silicate adsorbents by simultaneous inorganic-organic functionalization of low-grade palygorskite clay for removal of Congo red. Microporous and Mesoporous Materials, 2019, 277, 267-276.	4.4	49
279	Identifying key mononuclear Fe species for low-temperature methane oxidation. Chemical Science, 2021, 12, 3152-3160.	7.4	49
280	Preparation and swelling properties of pHâ€sensitive sodium alginate/layered double hydroxides hybrid beads for controlled release of diclofenac sodium. Journal of Biomedical Materials Research - Part B Applied Biomaterials, 2010, 92B, 205-214.	3.4	48
281	Attapulgite/Poly(acrylic acid) Nanocomposite (ATP/PAA) Hydrogels with Multifunctionalized Attapulgite (org-ATP) Nanorods as Unique Cross-linker: Preparation Optimization and Selective Adsorption of Pb(II) Ion. ACS Sustainable Chemistry and Engineering, 2014, 2, 643-651.	6.7	48
282	Novel Covalently Cross-Linked Attapulgite/Poly(acrylic acid- <i>co</i> -acrylamide) Hybrid Hydrogels by Inverse Suspension Polymerization: Synthesis Optimization and Evaluation as Adsorbents for Toxic Heavy Metals. Industrial & Engineering Chemistry Research, 2014, 53, 4277-4285.	3.7	48
283	Catalytic conversion of cellulosic biomass to ethylene glycol: Effects of inorganic impurities in biomass. Bioresource Technology, 2015, 175, 424-429.	9.6	48
284	Interconnected superporous adsorbent prepared via yeast-based Pickering HIPEs for high-efficiency adsorption of Rb+, Cs+ and Sr2+. Chemical Engineering Journal, 2019, 361, 1411-1422.	12.7	48
285	Incorporation of quaternary ammonium chitooligosaccharides on ZnO/palygorskite nanocomposites for enhancing antibacterial activities. Carbohydrate Polymers, 2020, 247, 116685.	10.2	48
286	Preparation and Swelling Behavior of Fast-Swelling Superabsorbent Hydrogels Based On Starch-g-Poly(acrylic acid-co-sodium acrylate). Macromolecular Materials and Engineering, 2006, 291, 612-620.	3.6	47
287	A Novel <i>N</i> â€&uccinylchitosanâ€ <i>graft</i> â€Polyacrylamide/Attapulgite Composite Hydrogel Prepared through Inverse Suspension Polymerization. Macromolecular Materials and Engineering, 2007, 292, 962-969.	3.6	47
288	Synthesis and Catalytic Performance of Highly Ordered Ru-Containing Mesoporous Carbons for Hydrogenation of Cinnamaldehyde. Catalysis Letters, 2008, 125, 289-295.	2.6	47

#	Article	IF	CITATIONS
289	Facile preparation of magnetic 2-hydroxypropyltrimethyl ammonium chloride chitosan/Fe3O4/halloysite nanotubes microspheres for the controlled release of ofloxacin. Carbohydrate Polymers, 2014, 102, 877-883.	10.2	47
290	Preparation, characterization and application on dye adsorption of a well-defined two-dimensional superparamagnetic clay/polyaniline/Fe3O4 nanocomposite. Applied Clay Science, 2016, 132-133, 7-16.	5.2	47
291	Highly efficient self-template synthesis of porous silica nanorods from natural palygorskite. Powder Technology, 2019, 354, 1-10.	4.2	47
292	ReO <sub><i>x</i></sub> /AC-Catalyzed Cleavage of C–O Bonds in Lignin Model Compounds and Alkaline Lignins. ACS Sustainable Chemistry and Engineering, 2019, 7, 208-215.	6.7	47
293	Recent Developments in Metal-Based Catalysts for the Catalytic Aerobic Oxidation of 5-Hydroxymethyl-Furfural to 2,5-Furandicarboxylic Acid. Catalysts, 2020, 10, 120.	3.5	47
294	Expression of survivin and correlation with PCNA in osteosarcoma. Journal of Surgical Oncology, 2006, 93, 578-584.	1.7	46
295	Synthesis, characterization and swelling behaviors of hydroxyethyl celluloseâ€∢i>gâ€poly(acrylic) Tj ETQq1 1	0.784314 3.1	rgBT /Overic
296	Facile self-assembly of Au nanoparticles on a magnetic attapulgite/Fe3O4 composite for fast catalytic decoloration of dye. RSC Advances, 2013, 3, 11515.	3.6	46
297	Acetylated modification of kapok fiber and application for oil absorption. Fibers and Polymers, 2013, 14, 1834-1840.	2.1	46
298	Highly efficient adsorption of Hg(II) and Pb(II) onto chitosan-based granular adsorbent containing thiourea groups. Journal of Water Process Engineering, 2015, 7, 218-226.	5.6	46
299	Pd/ZnO catalysts with different origins for high chemoselectivity in acetylene semi-hydrogenation. Chinese Journal of Catalysis, 2016, 37, 692-699.	14.0	46
300	Chemoselective hydrogenation of 3-nitrostyrene over a Pt/FeO <sub>x</sub> pseudo-single-atom-catalyst in CO <sub>2</sub> -expanded liquids. Green Chemistry, 2016, 18, 1332-1338.	9.0	46
301	Catalytic Conversion of Carbohydrates to Methyl Lactate Using Isolated Tin Sites in SBAâ€15. ChemistrySelect, 2017, 2, 309-314.	1.5	46
302	ls oxidation–reduction a real robust strategy for lignin conversion? A comparative study on lignin and model compounds. Green Chemistry, 2019, 21, 803-811.	9.0	46
303	Preparation and slow-release property of a poly(acrylic acid)/attapulgite/sodium humate superabsorbent composite. Journal of Applied Polymer Science, 2007, 103, 37-45.	2.6	45
304	Preparation and properties of chitosan/poly (vinyl alcohol) nanocomposite films reinforced with rod-like sepiolite. Materials Letters, 2012, 86, 69-72.	2.6	45
305	RuO <sub>2</sub> /rutile-TiO <sub>2</sub> : a superior catalyst for N <sub>2</sub> O decomposition. Journal of Materials Chemistry A, 2014, 2, 5178-5181.	10.3	45
306	Selective hydrogenation of acetylene in an ethylene-rich stream over silica supported Ag-Ni bimetallic catalysts. Applied Catalysis A: General, 2017, 545, 90-96.	4.3	45

#	Article	IF	CITATIONS
307	A comparative study of different natural palygorskite clays for fabricating cost-efficient and eco-friendly iron red composite pigments. Applied Clay Science, 2019, 167, 50-59.	5.2	45
308	Preparation and Ammonium Adsorption Properties of Biotite-Based Hydrogel Composites. Industrial & Engineering Chemistry Research, 2010, 49, 6034-6041.	3.7	44
309	Adsorption Characteristics of Chitosan- <i>g</i> Poly(acrylic acid)/Attapulgite Hydrogel Composite for Hg(II) Ions from Aqueous Solution. Separation Science and Technology, 2010, 45, 2086-2094.	2.5	44
310	Dramatically Enhanced Luminescence of Layered Terbium Hydroxides as Induced by the Synergistic Effect of Gd <sup>3+</sup> and Organic Sensitizers. Journal of Physical Chemistry C, 2014, 118, 14511-14520.	3.1	44
311	Enhanced Adsorptive Removal of Methylene Blue from Aqueous Solution by Alkali-Activated Palygorskite. Water, Air, and Soil Pollution, 2015, 226, 1.	2.4	44
312	Double biomimetic fabrication of robustly superhydrophobic cotton fiber and its application in oil spill cleanup. Industrial Crops and Products, 2015, 77, 36-43.	5.2	44
313	Dualâ€bed catalyst system for the direct synthesis of high density aviation fuel with cyclopentanone from lignocellulose. AICHE Journal, 2016, 62, 2754-2761.	3.6	44
314	A pH-sensitive composite hydrogel based on sodium alginate and medical stone: Synthesis, swelling, and heavy metal ions adsorption properties. Macromolecular Research, 2011, 19, 739-748.	2.4	43
315	Effects of solvent treatment and high-pressure homogenization process on dispersion properties of palygorskite. Powder Technology, 2013, 235, 652-660.	4.2	43
316	Selective hydrogenolysis of glycerol to 1,3-propanediol over Pt-W based catalysts. Chinese Journal of Catalysis, 2020, 41, 1311-1319.	14.0	43
317	Zeoliteâ€Tailored Active Site Proximity for the Efficient Production of Pentanoic Biofuels. Angewandte Chemie - International Edition, 2021, 60, 23713-23721.	13.8	43
318	Catalytic Performance of Activated Carbon Supported Tungsten Carbide for Hydrazine Decomposition. Catalysis Letters, 2008, 123, 150-155.	2.6	42
319	Synthesis of Renewable Triketones, Diketones, and Jetâ€Fuel Range Cycloalkanes with 5â€Hydroxymethylfurfural and Ketones. ChemSusChem, 2017, 10, 711-719.	6.8	42
320	Synthesis and Swelling Properties of Guar Gum-g-poly(sodium acrylate)/ Na-montmorillonite Superabsorbent Nanocomposite. Journal of Composite Materials, 2009, 43, 2805-2819.	2.4	41
321	XRF and nitrogen adsorption studies of acid-activated palygorskite. Clay Minerals, 2010, 45, 145-156.	0.6	41
322	Preparation of magnetic attapulgite nanocomposite for the adsorption of Ag+ and application for catalytic reduction of 4-nitrophenol. Journal of Materials Chemistry A, 2013, 1, 7083.	10.3	41
323	Synthesis of jet fuel range cycloalkanes with diacetone alcohol from lignocellulose. Green Chemistry, 2016, 18, 5751-5755.	9.0	41
324	More active Ir subnanometer clusters than singleâ€atoms for catalytic oxidation of CO at low temperature. AICHE Journal, 2017, 63, 4003-4012.	3.6	41

#	Article	IF	CITATIONS
325	Induction of apoptosis in K562 cells by jolkinolide B. Canadian Journal of Physiology and Pharmacology, 2006, 84, 959-965.	1.4	40
326	Nitrate Adsorption Using Poly(dimethyl diallyl ammonium chloride)/Polyacrylamide Hydrogel. Journal of Chemical & Engineering Data, 2010, 55, 3494-3500.	1.9	40
327	Ammonium sulfide-assisted hydrothermal activation of palygorskite for enhanced adsorption of methyl violet. Journal of Environmental Sciences, 2016, 41, 33-43.	6.1	40
328	ZnAlâ€Hydrotalciteâ€5upported Au <sub>25</sub> Nanoclusters as Precatalysts for Chemoselective Hydrogenation of 3â€Nitrostyrene. Angewandte Chemie, 2017, 129, 2753-2757.	2.0	40
329	Effect of oxalic acid-leaching levels on structure, color and physico-chemical features of palygorskite. Applied Clay Science, 2019, 183, 105301.	5.2	40
330	Mesoporous silicate/carbon composites derived from dye-loaded palygorskite clay waste for efficient removal of organic contaminants. Science of the Total Environment, 2019, 696, 133955.	8.0	40
331	Adsorption of cationic dye on N,O-carboxymethyl-chitosan from aqueous solutions: equilibrium, kinetics, and adsorption mechanism. Polymer Bulletin, 2010, 65, 961-975.	3.3	39
332	Synthesis of diesel range alkanes with 2-methylfuran and mesityl oxide from lignocellulose. Catalysis Today, 2014, 234, 91-99.	4.4	39
333	Learning from ancient Maya: Preparation of stable palygorskite/methylene blue@SiO2 Maya Blue-like pigment. Microporous and Mesoporous Materials, 2015, 211, 124-133.	4.4	39
334	Effect of grinding time on fabricating a stable methylene blue/palygorskite hybrid nanocomposite. Powder Technology, 2015, 280, 173-179.	4.2	39
335	From illite/smectite clay to mesoporous silicate adsorbent for efficient removal of chlortetracycline from water. Journal of Environmental Sciences, 2017, 51, 31-43.	6.1	39
336	Selective Production of Renewable <i>para</i> â€Xylene by Tungsten Carbide Catalyzed Atomâ€Economic Cascade Reactions. Angewandte Chemie - International Edition, 2018, 57, 1808-1812.	13.8	39
337	Co3+-O-V4+ cluster in CoVOx nanorods for efficient and stable electrochemical oxygen evolution. Applied Catalysis B: Environmental, 2021, 282, 119571.	20.2	39
338	Preparation of Cobalt Nitride from Co–Al Hydrotalcite and its Application in Hydrazine Decomposition. Topics in Catalysis, 2009, 52, 1535-1540.	2.8	38
339	A chitosan/poly(vinyl alcohol) nanocomposite film reinforced with natural halloysite nanotubes. Polymer Composites, 2012, 33, 1693-1699.	4.6	38
340	High Clay-Content Attapulgite/Poly(acrylic acid) Nanocomposite Hydrogel via Surface-Initiated Redox Radical Polymerization with Modified Attapulgite Nanorods as Initiator and Cross-Linker. Industrial & Engineering Chemistry Research, 2014, 53, 2067-2071.	3.7	38
341	Microwave-assisted fast conversion of lignin model compounds and organosolv lignin over methyltrioxorhenium in ionic liquids. RSC Advances, 2015, 5, 84967-84973.	3.6	38
342	Palygorskite@Fe <sub>3</sub> O <sub>4</sub> @polyperfluoroalkylsilane nanocomposites for superoleophobic coatings and magnetic liquid marbles. Journal of Materials Chemistry A, 2016, 4, 5859-5868.	10.3	38

#	Article	IF	CITATIONS
343	MgO/palygorskite adsorbent derived from natural Mg-rich brine and palygorskite for high-efficient removal of Cd(II) and Zn(II) ions. Journal of Environmental Chemical Engineering, 2017, 5, 1027-1036.	6.7	38
344	Ethylene glycol production from glucose over Wâ€Ru catalysts: Maximizing yield by kinetic modeling and simulation. AICHE Journal, 2017, 63, 2072-2080.	3.6	38
345	Recent researches on natural pigments stabilized by clay minerals: A review. Dyes and Pigments, 2021, 190, 109322.	3.7	38
346	A nanoporous hydrogel based on vinyl-functionalized alginate for efficient absorption and removal of Pb2+ ions. International Journal of Biological Macromolecules, 2013, 62, 225-231.	7.5	37
347	Supported Au-Ni nano-alloy catalysts for the chemoselective hydrogenation of nitroarenes. Chinese Journal of Catalysis, 2015, 36, 160-167.	14.0	37
348	Industrially scalable and cost-effective synthesis of 1,3-cyclopentanediol with furfuryl alcohol from lignocellulose. Green Chemistry, 2016, 18, 3607-3613.	9.0	37
349	Synergistic effect of chitosan and halloysite nanotubes on improving agar film properties. Food Hydrocolloids, 2020, 101, 105471.	10.7	37
350	Study on superabsorbent composites. XXI. Synthesis, characterization and swelling behaviors of chitosanâ€ <i>g</i> â€poly(acrylic acid)/organoâ€rectorite nanocomposite superabsorbents. Journal of Applied Polymer Science, 2008, 110, 678-686.	2.6	36
351	Preparation and properties of kapok fiber enhanced oil sorption resins by suspended emulsion polymerization. Journal of Applied Polymer Science, 2013, 127, 2184-2191.	2.6	36
352	Production of Renewable Jet Fuel Range Branched Alkanes with Xylose and Methyl Isobutyl Ketone. Industrial & Engineering Chemistry Research, 2014, 53, 13618-13625.	3.7	36
353	All-into-one strategy to synthesize mesoporous hybrid silicate microspheres from naturally rich red palygorskite clay as high-efficient adsorbents. Scientific Reports, 2016, 6, 39599.	3.3	36
354	Fabrication of manganese dioxide/carbon/attapulgite composites derived from spent bleaching earth for adsorption of Pb( <scp>ii</scp> ) and Brilliant green. RSC Advances, 2016, 6, 36534-36543.	3.6	36
355	Pt/Nb-WO x for the chemoselective hydrogenolysis of glycerol to 1,3-propanediol: Nb dopant pacifying the over-reduction of WO x supports. Chinese Journal of Catalysis, 2018, 39, 1027-1037.	14.0	36
356	Durable Superhydrophobic Surfaces Prepared by Spray Coating of Polymerized Organosilane/Attapulgite Nanocomposites. ChemPlusChem, 2013, 78, 1503-1509.	2.8	35
357	Non-covalently functionalized multiwalled carbon nanotubes by chitosan and their synergistic reinforcing effects in PVA films. RSC Advances, 2013, 3, 1210-1216.	3.6	35
358	Synthesis of polyaniline/carbon black hybrid hollow microspheres by layer-by-layer assembly used as electrode materials for supercapacitors. Electrochimica Acta, 2013, 88, 177-183.	5.2	35
359	Facile fabrication of carbon/attapulgite composite for bleaching of palm oil. Journal of the Taiwan Institute of Chemical Engineers, 2015, 50, 252-258.	5.3	35
360	Mesoporous hybrid Zn-silicate derived from red palygorskite clay as a high-efficient adsorbent for antibiotics. Microporous and Mesoporous Materials, 2016, 234, 317-325.	4.4	35

#	Article	IF	CITATIONS
361	Highly efficient synthesis of 5-hydroxymethylfurfural with carbohydrates over renewable cyclopentanone-based acidic resin. Green Chemistry, 2017, 19, 1855-1860.	9.0	35
362	Oriented growth of poly(m-phenylenediamine) on Calotropis gigantea fiber for rapid adsorption of ciprofloxacin. Chemosphere, 2017, 171, 223-230.	8.2	35
363	Calotropis gigantea fiber derived carbon fiber enables fast and efficient absorption of oils and organic solvents. Separation and Purification Technology, 2018, 192, 30-35.	7.9	35
364	Effects of divalent metal ions of hydrotalcites on catalytic behavior of supported gold nanocatalysts for chemoselective hydrogenation of 3-nitrostyrene. Journal of Catalysis, 2018, 364, 174-182.	6.2	35
365	Preparation, swelling behaviors and application of polyacrylamide/attapulgite superabsorbent composites. Polymers for Advanced Technologies, 2006, 17, 12-19.	3.2	34
366	Synthesis, characterization, and catalytic application of highly ordered mesoporous alumina-carbon nanocomposites. Nano Research, 2011, 4, 50-60.	10.4	34
367	Au nanoparticles decorated Kapok fiber by a facile noncovalent approach for efficient catalytic decoloration of Congo Red and hydrogen production. Chemical Engineering Journal, 2014, 237, 336-343.	12.7	34
368	Tailoring the properties of palygorskite by various organic acids via a one-pot hydrothermal process: A comparative study for removal of toxic dyes. Applied Clay Science, 2016, 120, 28-39.	5.2	34
369	A comparative study for oil-absorbing performance of octadecyltrichlorosilane treated Calotropis gigantea fiber and kapok fiber. Cellulose, 2017, 24, 989-1000.	4.9	34
370	Three-dimensional hollow microtubular carbonized kapok fiber/cobalt-nickel binary oxide composites for high-performance electrode materials of supercapacitors. Electrochimica Acta, 2017, 224, 113-124.	5.2	34
371	Evaluation of Ce(III) and Gd(III) adsorption from aqueous solution using CTS- g -(AA- co -SS)/ISC hybrid hydrogel adsorbent. Journal of Rare Earths, 2017, 35, 697-708.	4.8	34
372	Cost-efficient, vivid and stable red hybrid pigments derived from naturally available sepiolite and halloysite. Ceramics International, 2017, 43, 1862-1869.	4.8	34
373	Effect of removing coloring metal ions from the natural brick-red palygorskite on properties of alginate/palygorskite nanocomposite film. International Journal of Biological Macromolecules, 2019, 122, 684-694.	7.5	34
374	Mesoporous polymetallic silicate derived from naturally abundant mixed clay: A potential robust adsorbent for removal of cationic dye and antibiotic. Powder Technology, 2021, 390, 303-314.	4.2	34
375	Effect of biotite content of hydrogels on enhanced removal of methylene blue from aqueous solution. lonics, 2011, 17, 535-543.	2.4	33
376	Preparation, swelling, and stimuliâ€responsive characteristics of superabsorbent nanocomposites based on carboxymethyl cellulose and rectorite. Polymers for Advanced Technologies, 2011, 22, 1602-1611.	3.2	33
377	pH-responsive sodium alginate-based superporous hydrogel generated by an anionic surfactant micelle templating. Carbohydrate Polymers, 2013, 94, 449-455.	10.2	33
378	Facile preparation of stable palygorskite/methyl violet@SiO2 "Maya Violet―pigment. Journal of Colloid and Interface Science, 2015, 457, 254-263.	9.4	33

#	Article	IF	CITATIONS
379	Direct synthesis of gasoline and diesel range branched alkanes with acetone from lignocellulose. Green Chemistry, 2016, 18, 3707-3711.	9.0	33
380	Cobalt blue hybrid pigment doped with magnesium derived from sepiolite. Applied Clay Science, 2018, 157, 111-120.	5.2	33
381	A novel graphene aerogel synthesized from cellulose with high performance for removing MB in water. Journal of Materials Science and Technology, 2020, 41, 68-75.	10.7	33
382	A superabsorbent nanocomposite based on sodium alginate and illite/smectite mixedâ€layer clay. Journal of Applied Polymer Science, 2013, 130, 161-167.	2.6	32
383	Fabrication of attapulgite/carbon composites from spent bleaching earth for the efficient adsorption of methylene blue. RSC Advances, 2015, 5, 38443-38451.	3.6	32
384	In situ generation of silver nanoparticles within crosslinked 3D guar gum networks for catalytic reduction. International Journal of Biological Macromolecules, 2015, 73, 39-44.	7.5	32
385	Synthesis of renewable diesel with 2-methylfuran and angelica lactone derived from carbohydrates. Green Chemistry, 2016, 18, 1218-1223.	9.0	32
386	Modulating <i>trans</i> -imination and hydrogenation towards the highly selective production of primary diamines from dialdehydes. Green Chemistry, 2020, 22, 6897-6901.	9.0	32
387	Fabrication porous adsorbents templated from modified sepiolite-stabilized aqueous foams for high-efficient removal of cationic dyes. Chemosphere, 2020, 259, 126949.	8.2	32
388	Study on Superabsorbent Composite, 14. Macromolecular Materials and Engineering, 2006, 291, 1529-1538.	3.6	31
389	Visible light sensitized attapulgite-based lanthanide composites: microstructure, photophysical behaviour and biological application. Dalton Transactions, 2011, 40, 12909.	3.3	31
390	Enhanced swelling properties of a novel sodium alginateâ€based superabsorbent composites: NaAlgâ€ <i>g</i> â€poly(NaAâ€ <i>co</i> â€St)/APT. Journal of Applied Polymer Science, 2012, 125, 1822-1832.	2.6	31
391	Enhanced swelling and responsive properties of an alginate-based superabsorbent hydrogel by sodium p-styrenesulfonate and attapulgite nanorods. Polymer Bulletin, 2013, 70, 1181-1193.	3.3	31
392	Catalytically Active Rh Subâ€Nanoclusters on TiO <sub>2</sub> for CO Oxidation at Cryogenic Temperatures. Angewandte Chemie, 2016, 128, 2870-2874.	2.0	31
393	Production of renewable 1,3-pentadiene from xylitol via formic acid-mediated deoxydehydration and palladium-catalyzed deoxygenation reactions. Green Chemistry, 2017, 19, 638-642.	9.0	31
394	Solvothermal evolution of red palygorskite in dimethyl sulfoxide/water. Applied Clay Science, 2018, 159, 16-24.	5.2	31
395	Low-cost bismuth yellow hybrid pigments derived from attapulgite. Dyes and Pigments, 2018, 149, 521-530.	3.7	31
396	High-loading and thermally stable Pt1/MgAl1.2Fe0.8O4 single-atom catalysts for high-temperature applications. Science China Materials, 2020, 63, 949-958.	6.3	31

#	Article	IF	CITATIONS
397	From structure evolution of palygorskite to functional material: A review. Microporous and Mesoporous Materials, 2022, 333, 111765.	4.4	31
398	Superparamagnetic sandwich structured silver/halloysite nanotube/Fe <sub>3</sub> O <sub>4</sub> nanocomposites for 4-nitrophenol reduction. RSC Advances, 2014, 4, 39439-39445.	3.6	30
399	From naturally low-grade palygorskite to hybrid silicate adsorbent for efficient capture of Cu(II) ions. Applied Clay Science, 2016, 132-133, 438-448.	5.2	30
400	Palygorskite in sodium sulphide solution via hydrothermal process for enhanced methylene blue adsorption. Journal of the Taiwan Institute of Chemical Engineers, 2016, 58, 417-423.	5.3	30
401	Dehydration of Carbohydrates to 5-Hydroxymethylfurfural over Lignosulfonate-Based Acidic Resin. ACS Sustainable Chemistry and Engineering, 2018, 6, 5645-5652.	6.7	30
402	Synthesis of jet fuel range high-density polycycloalkanes with polycarbonate waste. Green Chemistry, 2019, 21, 3789-3795.	9.0	30
403	Understanding the deactivation behavior of Pt/WO3/Al2O3 catalyst in the glycerol hydrogenolysis reaction. Chinese Journal of Catalysis, 2020, 41, 1261-1267.	14.0	30
404	Manipulated dispersion of carbon nanotubes with derivatives of chitosan. Carbon, 2007, 45, 1917-1920.	10.3	29
405	Adsorption properties of Cu(II) ions onto N-succinyl-chitosan and crosslinked N-succinyl-chitosan template resin. Biochemical Engineering Journal, 2007, 36, 131-138.	3.6	29
406	Study on superabsorbent composite. XI. Effect of thermal treatment and acid activation of attapulgite on water absorbency of poly(acrylic acid)/attapulgite superabsorbent composite. Polymer Composites, 2007, 28, 397-404.	4.6	29
407	Microwave-Assisted Preparation and Hydrazine Decomposition Properties of Nanostructured Tungsten Carbides on Carbon Nanotubes. Industrial & Engineering Chemistry Research, 2009, 48, 3244-3248.	3.7	29
408	Removal of Cd(II) from aqueous solution by a composite hydrogel based on attapulgite. Environmental Technology (United Kingdom), 2010, 31, 745-753.	2.2	29
409	Synthesis and enhanced swelling properties of a guar gum-based superabsorbent composite by the simultaneous introduction of styrene and attapulgite. Journal of Polymer Research, 2011, 18, 1705-1713.	2.4	29
410	H <sub>2</sub> production by selective decomposition of hydrous hydrazine over Raney Ni catalyst under ambient conditions. AICHE Journal, 2013, 59, 4297-4302.	3.6	29
411	In situ fabrication of Ag nanoparticles/attapulgite nanocomposites: green synthesis and catalytic application. Journal of Nanoparticle Research, 2014, 16, 1.	1.9	29
412	Facile fabrication of superparamagnetic coaxial gold/halloysite nanotubes/Fe3O4 nanocomposites with excellent catalytic property for 4-nitrophenol reduction. Journal of Materials Science, 2014, 49, 7181-7191.	3.7	29
413	High-pressure homogenization associated hydrothermal process of palygorskite for enhanced adsorption of Methylene blue. Applied Surface Science, 2015, 329, 306-314.	6.1	29
414	Feâ€substituted Baâ€hexaaluminates oxygen carrier for carbon dioxide capture by chemical looping combustion of methane. AICHE Journal, 2016, 62, 792-801.	3.6	29

#	Article	IF	CITATIONS
415	Synthesis of Renewable C <sub>8</sub> –C <sub>10</sub> Alkanes with Angelica Lactone and Furfural from Carbohydrates. ACS Sustainable Chemistry and Engineering, 2018, 6, 6126-6134.	6.7	29
416	Attapulgite/carbon composites as a recyclable adsorbent for antibiotics removal. Korean Journal of Chemical Engineering, 2018, 35, 1650-1661.	2.7	29
417	Synthesis of high-density aviation fuels with methyl benzaldehyde and cyclohexanone. Green Chemistry, 2018, 20, 3753-3760.	9.0	29
418	Recent researches on antimicrobial nanocomposite and hybrid materials based on sepiolite and palygorskite. Applied Clay Science, 2022, 219, 106454.	5.2	29
419	Preparation, Swelling, and Slow-Release Characteristics of Superabsorbent Composite Containing Sodium Humate. Industrial & Engineering Chemistry Research, 2008, 47, 1766-1773.	3.7	28
420	Superabsorbent composite XXII: Effects of modified sepiolite on water absorbency and swelling behavior of chitosanâ€ <i>g</i> â€poly(acrylic acid)/sepiolite superabsorbent composite. Polymer Composites, 2010, 31, 89-96.	4.6	28
421	Adsorption Behavior of Methylene Blue from Aqueous Solution by the Hydrogel Composites Based on Attapulgite. Separation Science and Technology, 2011, 46, 858-868.	2.5	28
422	Template synthesis of graphene/polyaniline hybrid hollow microspheres as electrode materials for high-performance supercapacitor. Journal of Nanoparticle Research, 2014, 16, 1.	1.9	28
423	Effects of solvothermal process on the physicochemical and adsorption characteristics of palygorskite. Applied Clay Science, 2015, 107, 230-237.	5.2	28
424	From nanorods of palygorskite to nanosheets of smectite via a one-step hydrothermal process. RSC Advances, 2015, 5, 58107-58115.	3.6	28
425	Effect of promoters on the selective hydrogenolysis of glycerol over Pt/W-containing catalysts. Chinese Journal of Catalysis, 2016, 37, 1513-1519.	14.0	28
426	Tungsten-based catalysts for lignin depolymerization: the role of tungsten species in C–O bond cleavage. Catalysis Science and Technology, 2019, 9, 2144-2151.	4.1	28
427	Recent advances in the potential applications of hollow kapok fiber-based functional materials. Cellulose, 2021, 28, 5269-5292.	4.9	28
428	Cu <sup>2+</sup> removal from aqueous solution by modified chitosan hydrogels. Journal of Chemical Technology and Biotechnology, 2012, 87, 1010-1016.	3.2	27
429	Improving capacitance performance of attapulgite/polypyrrole composites by introducing rhodamine B. Electrochimica Acta, 2013, 89, 422-428.	5.2	27
430	Dispersion of palygorskite in ethanol–water mixtures via high-pressure homogenization: Microstructure and colloidal properties. Powder Technology, 2014, 261, 98-104.	4.2	27
431	Selective removal of 1,2â€propanediol and 1,2â€butanediol from bioâ€ethylene glycol by catalytic reaction. AICHE Journal, 2017, 63, 4032-4042.	3.6	27
432	Metallic nanoparticles roughened Calotropis gigantea fiber enables efficient absorption of oils and organic solvents. Industrial Crops and Products, 2018, 115, 272-279.	5.2	27

#	Article	IF	CITATIONS
433	Effects of modification of palygorskite on superamphiphobicity and microstructure of palygorskite@fluorinated polysiloxane superamphiphobic coatings. Applied Clay Science, 2018, 160, 144-152.	5.2	27
434	Optimal Synthesis of Environment-Friendly Iron Red Pigment from Natural Nanostructured Clay Minerals. Nanomaterials, 2018, 8, 925.	4.1	27
435	From waste hot-pot oil as carbon precursor to development of recyclable attapulgite/carbon composites for wastewater treatment. Journal of Environmental Sciences, 2019, 75, 346-358.	6.1	27
436	<p>A Novel 3D-bioprinted Porous Nano Attapulgite Scaffolds with Good Performance for Bone Regeneration</p> . International Journal of Nanomedicine, 2020, Volume 15, 6945-6960.	6.7	27
437	Catalytic production of 1,4-pentanediol from furfural in a fixed-bed system under mild conditions. Green Chemistry, 2020, 22, 3532-3538.	9.0	27
438	Removal of antibiotics from aqueous solution by using porous adsorbent templated from eco-friendly Pickering aqueous foams. Journal of Environmental Sciences, 2021, 102, 352-362.	6.1	27
439	Synthesis of bio-based methylcyclopentadiene via direct hydrodeoxygenation of 3-methylcyclopent-2-enone derived from cellulose. Nature Communications, 2021, 12, 46.	12.8	27
440	Superoxide anion: Critical source of high performance antibacterial activity in Co-Doped ZnO QDs. Ceramics International, 2020, 46, 15822-15830.	4.8	27
441	Synthesis, characterization and swelling properties of guar gum- <i>g</i> -poly(sodium) Tj ETQq1 1 0.784314 rgBT Advanced Materials, 2010, 11, 025006.	/Overlock 6.1	10 Tf 50 4 26
442	Electrokinetic and Colloidal Properties of Homogenized and Unhomogenized Palygorskite in the Presence of Electrolytes. Journal of Chemical & Engineering Data, 2012, 57, 1586-1593.	1.9	26
443	Facile hydrothermal synthesis of tubular kapok fiber/MnO <sub>2</sub> composites and application in supercapacitors. RSC Advances, 2015, 5, 64065-64075.	3.6	26
444	Hollowed-out tubular carbon@MnO 2 hybrid composites with controlled morphology derived from kapok fibers for supercapacitor electrode materials. Electrochimica Acta, 2015, 178, 709-720.	5.2	26
445	Synthesis of 1,4 yclohexanedimethanol, 1,4 yclohexanedicarboxylic Acid and 1,2 yclohexanedicarboxylates from Formaldehyde, Crotonaldehyde and Acrylate/Fumarate. Angewandte Chemie - International Edition, 2018, 57, 6901-6905.	13.8	26
446	A facile approach to fabricate bright blue heat-resisting paint with self-cleaning ability based on CoAl 2 O 4 /kaolin hybrid pigment. Applied Clay Science, 2018, 160, 153-161.	5.2	26
447	Embedding CsPbBr <sub>3</sub> quantum dots into a pillar[5]arene-based supramolecular self-assembly for an efficient photocatalytic cross-coupling hydrogen evolution reaction. Journal of Materials Chemistry A, 2021, 9, 10180-10185.	10.3	26
448	Promoting the Effect of Au on the Selective Hydrogenolysis of Glycerol to 1,3-Propanediol over the Pt/WO <sub><i>x</i></sub> /Al <sub>2</sub> O <sub>3</sub> Catalyst. ACS Sustainable Chemistry and Engineering, 2021, 9, 5705-5715.	6.7	26
449	Catalytic production of low-carbon footprint sustainable natural gas. Nature Communications, 2022, 13, 258.	12.8	26
450	Study on superabsorbent composite—VII. Effects of organification of attapulgite on swelling behaviors of poly(acrylic acid-co-acrylamide)/sodium humate/organo-attapulgite composite. Polymers for Advanced Technologies, 2006, 17, 379-385.	3.2	25

#	Article	IF	CITATIONS
451	Facile Synthesis of Ultrathin AuCu Dimetallic Nanowire Networks. European Journal of Inorganic Chemistry, 2012, 2012, 2700-2706.	2.0	25
452	Spray-dried magnetic chitosan/Fe3O4/halloysite nanotubes/ofloxacin microspheres for sustained release of ofloxacin. RSC Advances, 2013, 3, 23423.	3.6	25
453	Freeze-drying: A versatile method to overcome re-aggregation and improve dispersion stability of palygorskite for sustained release of ofloxacin. Applied Clay Science, 2014, 87, 7-13.	5.2	25
454	Ethanol–NaOH solidification method to intensify chitosan/poly(vinyl alcohol)/attapulgite composite film. RSC Advances, 2015, 5, 17775-17781.	3.6	25
455	Effect of different clay minerals and calcination temperature on the morphology and color of clay/CoAl <sub>2</sub> O <sub>4</sub> hybrid pigments. RSC Advances, 2015, 5, 102674-102681.	3.6	25
456	Synthesis of jet fuel range branched cycloalkanes with mesityl oxide and 2-methylfuran from lignocellulose. Scientific Reports, 2016, 6, 32379.	3.3	25
457	A two-step synthesis of Fe-substituted hexaaluminates with enhanced surface area and activity in methane catalytic combustion. Catalysis Science and Technology, 2016, 6, 4962-4969.	4.1	25
458	Experimental investigation and theoretical exploration of single-atom electrocatalysis in hybrid photovoltaics: The powerful role of Pt atoms in triiodide reduction. Nano Energy, 2017, 39, 1-8.	16.0	25
459	Preparation and cyclic utilization assessment of palygorskite/carbon composites for sustainable efficient removal of methyl violet. Applied Clay Science, 2018, 161, 317-325.	5.2	25
460	Reactivity of Methanol Steam Reforming on ZnPd Intermetallic Catalyst: Understanding from Microcalorimetric and FT-IR Studies. Journal of Physical Chemistry C, 2018, 122, 12395-12403.	3.1	25
461	Acid/base reversible allochroic anthocyanin/palygorskite hybrid pigments: Preparation, stability and potential applications. Dyes and Pigments, 2019, 171, 107738.	3.7	25
462	One-pot synthesis of novel hierarchically porous and hydrophobic Si/SiOx composite from natural palygorskite for benzene adsorption. Chemical Engineering Journal, 2019, 378, 122131.	12.7	25
463	A Comparative Study on Color Stability of Anthocyanin Hybrid Pigments Derived from 1D and 2D Clay Minerals. Materials, 2019, 12, 3287.	2.9	25
464	Tunable superporous magnetic adsorbent prepared via eco-friendly Pickering MIPEs for high-efficiency adsorption of Rb+ and Sr2+. Chemical Engineering Journal, 2019, 368, 988-998.	12.7	25
465	Magnetic nano-hybrids adsorbents formulated from acidic leachates of clay minerals. Journal of Cleaner Production, 2020, 256, 120383.	9.3	25
466	pH- and thermo-responsive dispersion of single-walled carbon nanotubes modified with poly(N-isopropylacrylamide-co-acrylic acid). Journal of Colloid and Interface Science, 2009, 334, 212-216.	9.4	24
467	Synthesis, characterization and swelling behaviors of guar gum- <i>g</i> -poly(sodium) Tj ETQq1 1 0.784314 rgBT 2011, 45, 2189-2198.	/Overlock 2.4	10 Tf 50 1 24
468	Universal self-assembly of organosilanes with long alkyl groups into silicone nanofilaments. Polymer Chemistry, 2014, 5, 1132-1139.	3.9	24

#	Article	IF	CITATIONS
469	Ag(I)-triggered one-pot synthesis of Ag nanoparticles onto natural nanorods as a multifunctional nanocomposite for efficient catalysis and adsorption. Journal of Colloid and Interface Science, 2016, 473, 84-92.	9.4	24
470	Pd1/CeO2 single-atom catalyst for alkoxycarbonylation of aryl iodides. Science China Materials, 2020, 63, 959-964.	6.3	24
471	SYNTHESIS OFMESO-ARYLSUBSTITUTED CALIX[4]PYRROLES. Synthetic Communications, 2001, 31, 1421-1426.	2.1	23
472	Effects of modified vermiculite on the synthesis and swelling behaviors of hydroxyethyl cellulose-g-poly(acrylic acid)/vermiculite superabsorbent nanocomposites. Journal of Polymer Research, 2011, 18, 401-408.	2.4	23
473	Efficient Adsorption and Recovery of Pb(II) from Aqueous Solution by a Granular pH-Sensitive Chitosan-based Semi-IPN Hydrogel. Journal of Macromolecular Science - Pure and Applied Chemistry, 2012, 49, 971-979.	2.2	23
474	Highly Active Small Palladium Clusters Supported on Ferric Hydroxide for Carbon Monoxideâ€Tolerant Hydrogen Oxidation. ChemCatChem, 2014, 6, 547-554.	3.7	23
475	Ni(OH)2/MoS x nanocomposite electrodeposited on a flexible CNT/PI membrane as an electrochemical glucose sensor: the synergistic effect of Ni(OH)2 and MoS x. Journal of Solid State Electrochemistry, 2016, 20, 133-142.	2.5	23
476	Synthesis of renewable high-density fuel with isophorone. Scientific Reports, 2017, 7, 6111.	3.3	23
477	Insights into the relationship between the color and photocatalytic property of attapulgite/CdS nanocomposites. Applied Surface Science, 2018, 439, 202-212.	6.1	23
478	Reversible Thermochromic Superhydrophobic BiVO <sub>4</sub> Hybrid Pigments Coatings with Self-Cleaning Performance and Environmental Stability Based on Kaolinite. ACS Applied Materials & Interfaces, 2021, 13, 3228-3236.	8.0	23
479	Synthesis of iron red hybrid pigments from oil shale semi-coke waste. Advanced Powder Technology, 2020, 31, 2276-2284.	4.1	23
480	Crystallinity-Modulated Co <sub>2–<i>x</i></sub> V <sub><i>x</i></sub> O <sub>4</sub> Nanoplates for Efficient Electrochemical Water Oxidation. ACS Catalysis, 2021, 11, 14884-14891.	11.2	23
481	Introducing Co–O Moiety to Co–N–C Single-Atom Catalyst for Ethylbenzene Dehydrogenation. ACS Catalysis, 2022, 12, 7760-7772.	11.2	23
482	Effects of Modified Vermiculite on Water Absorbency and Swelling Behavior of Chitosan-g-Poly(Acrylic Acid)/Vermiculite Superabsorbent Composite. Journal of Composite Materials, 2009, 43, 2401-2417.	2.4	22
483	Superhydrophobic Gated Polyorganosilanes/Halloysite Nanocontainers for Sustained Drug Release. Advanced Materials Interfaces, 2014, 1, 1300136.	3.7	22
484	Solvatochromic Coatings with Self-Cleaning Property from Palygorskite@Polysiloxane/Crystal Violet Lactone. ACS Applied Materials & Interfaces, 2016, 8, 27346-27352.	8.0	22
485	Poly( m -phenylenediamine) functionalized Calotropis gigantea fiber for coupled adsorption reduction for Cr(VI). Journal of Molecular Liquids, 2017, 240, 225-232.	4.9	22
486	Synthesis of 1,4â€Cyclohexanedimethanol, 1,4â€Cyclohexanedicarboxylic Acid and 1,2â€Cyclohexanedicarboxylates from Formaldehyde, Crotonaldehyde and Acrylate/Fumarate. Angewandte Chemie, 2018, 130, 7017-7021.	2.0	22

#	Article	IF	CITATIONS
487	Superamphiphobic Coatings with Low Sliding Angles from Attapulgite/Carbon Composites. Advanced Materials Interfaces, 2018, 5, 1701520.	3.7	22
488	Carbon/Attapulgite Composites as Recycled Palm Oil-Decoloring and Dye Adsorbents. Materials, 2018, 11, 86.	2.9	22
489	Amine formylation with CO2 and H2 catalyzed by heterogeneous Pd/PAL catalyst. Chinese Journal of Catalysis, 2019, 40, 1141-1146.	14.0	22
490	Preparation of Carboxymethyl Cellulose-Based Macroporous Adsorbent by Eco-Friendly Pickering-MIPEs Template for Fast Removal of Pb2+ and Cd2+. Frontiers in Chemistry, 2019, 7, 603.	3.6	22
491	One-pot synthesis of polymer-reinforced silica aerogels from high internal phase emulsion templates. Journal of Colloid and Interface Science, 2020, 573, 62-70.	9.4	22
492	A pH-sensitive nanocomposite microsphere based on chitosan and montmorillonite with in vitro reduction of the burst release effect. Drug Development and Industrial Pharmacy, 2010, 36, 1106-1114.	2.0	21
493	Enhanced microscopic structure and properties of palygorskite by associated extrusion and high-pressure homogenization process. Applied Clay Science, 2014, 95, 365-370.	5.2	21
494	An evaluation of palygorskite inclusion on the growth performance and digestive function of broilers. Applied Clay Science, 2016, 129, 1-6.	5.2	21
495	Sustainable production of pyromellitic acid with pinacol and diethyl maleate. Green Chemistry, 2017, 19, 1663-1667.	9.0	21
496	Fabrication of porous adsorbent via eco-friendly Pickering-MIPEs polymerization for rapid removal of Rb+ and Cs+. Journal of Environmental Chemical Engineering, 2018, 6, 849-857.	6.7	21
497	Structure evolution of brick-red palygorskite induced by hydroxylammonium chloride. Powder Technology, 2018, 327, 246-254.	4.2	21
498	Synthesis of Decaline-Type Thermal-Stable Jet Fuel Additives with Cycloketones. ACS Sustainable Chemistry and Engineering, 2019, 7, 17354-17361.	6.7	21
499	Preparation of effective carvacrol/attapulgite hybrid antibacterial materials by mechanical milling. Journal of Porous Materials, 2020, 27, 843-853.	2.6	21
500	Granular hydrogel initiated by Fenton reagent and their performance on Cu(II) and Ni(II) removal. Chemical Engineering Journal, 2012, 200-202, 601-610.	12.7	20
501	Synthesis and oil absorption of poly(butylmethacrylate)/organoâ€attapulgite nanocomposite by suspended emulsion polymerization. Polymer Composites, 2013, 34, 274-281.	4.6	20
502	Superior dispersion properties of palygorskite in dimethyl sulfoxide via high-pressure homogenization process. Applied Clay Science, 2013, 86, 174-178.	5.2	20
503	A novel approach for dispersion palygorskite aggregates into nanorods via adding freezing process into extrusion and homogenization treatment. Powder Technology, 2013, 249, 157-162.	4.2	20
504	Attapulgite Modified with Silane Coupling Agent for Phosphorus Adsorption and Deep Bleaching of Refined Palm Oil. Adsorption Science and Technology, 2014, 32, 37-48.	3.2	20

#	Article	IF	CITATIONS
505	Attapulgite oriented carbon/polyaniline hybrid nanocomposites for electrochemical energy storage. Synthetic Metals, 2014, 192, 87-92.	3.9	20
506	Fabrication of a magnetic porous hydrogel sphere for efficient enrichment of Rb+ and Cs+ from aqueous solution. Chemical Engineering Research and Design, 2017, 125, 214-225.	5.6	20
507	Fabrication of CMC-g-PAM Superporous Polymer Monoliths via Eco-Friendly Pickering-MIPEs for Superior Adsorption of Methyl Violet and Methylene Blue. Frontiers in Chemistry, 2017, 5, 33.	3.6	20
508	Formation and Coloring Mechanism of Typical Aluminosilicate Clay Minerals for CoAl2O4 Hybrid Pigment Preparation. Frontiers in Chemistry, 2018, 6, 125.	3.6	20
509	Significantly improve the water and chemicals resistance of alginate-based nanocomposite films by a simple in-situ surface coating approach. International Journal of Biological Macromolecules, 2020, 156, 1297-1307.	7.5	20
510	Glucosamine sulfate–induced apoptosis in chronic myelogenous leukemia K562 cells is associated with translocation of cathepsin D and downregulation of Bcl-xL. Apoptosis: an International Journal on Programmed Cell Death, 2006, 11, 1851-1860.	4.9	19
511	Preparation and swelling properties of semiâ€IPN hydrogels based on chitosanâ€ <i>g</i> â€poly(acrylic acid) and phosphorylated polyvinyl alcohol. Journal of Applied Polymer Science, 2009, 114, 643-652.	2.6	19
512	Relationship between adsorption properties of Pt–Cu/SiO2 catalysts and their catalytic performance for selective hydrodechlorination of 1,2-dichloroethane to ethylene. Thermochimica Acta, 2009, 494, 99-103.	2.7	19
513	pH-sensitive magnetic alginate-chitosan beads for albendazole delivery. Pharmaceutical Development and Technology, 2011, 16, 228-236.	2.4	19
514	Preparation and swelling characteristics of a superabsorbent nanocomposite based on natural guar gum and cationâ€modified vermiculite. Journal of Applied Polymer Science, 2011, 119, 3675-3686.	2.6	19
515	Study on thermal activated sepiolite for enhancing decoloration of crude palm oil. Journal of Thermal Analysis and Calorimetry, 2014, 117, 1211-1219.	3.6	19
516	Porous carbon nanoflakes with a high specific surface area derived from a kapok fiber for high-performance electrode materials of supercapacitors. RSC Advances, 2016, 6, 6967-6977.	3.6	19
517	Facile synthesis of macroporous zwitterionic hydrogels templated from graphene oxide-stabilized aqueous foams. Journal of Colloid and Interface Science, 2019, 553, 40-49.	9.4	19
518	Microwave hydrothermal assisted preparation of CoAl2O4/kaolin hybrid pigments for reinforcement coloring and mechanical property of acrylonitrile butadiene styrene. Applied Clay Science, 2019, 175, 67-75.	5.2	19
519	Synthesis of jet fuel additive with cyclopentanone. Journal of Energy Chemistry, 2019, 29, 23-30.	12.9	19
520	Highâ€Đensity and Thermally Stable Palladium Singleâ€Atom Catalysts for Chemoselective Hydrogenations. Angewandte Chemie, 2020, 132, 21797-21803.	2.0	19
521	Direct Synthesis of Methylcyclopentadiene with 2,5-Hexanedione over Zinc Molybdates. ACS Catalysis, 2021, 11, 4810-4820.	11.2	19
522	Direct synthesis of a high-density aviation fuel using a polycarbonate. Green Chemistry, 2021, 23, 912-919.	9.0	19

#	Article	IF	CITATIONS
523	A Novel Route to the Preparation of Carbon Supported Nickel Phosphide Catalysts by a Microwave Heating Process. Catalysis Letters, 2010, 135, 305-311.	2.6	18
524	Preparation and swelling properties of a pHâ€sensitive superabsorbent hydrogel based on psyllium gum. Starch/Staerke, 2010, 62, 501-507.	2.1	18
525	Decorated resol derived mesoporous carbon: highly ordered microstructure, rich boron incorporation, and excellent electrochemical capacitance. RSC Advances, 2013, 3, 3578.	3.6	18
526	Enhanced Selectivity for Heavy Metals Using Polyaniline-Modified Hydrogel. Industrial & Engineering Chemistry Research, 2013, 52, 4957-4961.	3.7	18
527	Targeting of fluorescent palygorskite polyethyleneimine nanocomposite to cancer cells. Applied Clay Science, 2014, 101, 567-573.	5.2	18
528	Halloysite nanotubes induced synthesis of carbon/manganese dioxide coaxial tubular nanocomposites as electrode materials for supercapacitors. Journal of Solid State Electrochemistry, 2015, 19, 1257-1263.	2.5	18
529	Gelatin-Grafted Granular Composite Hydrogel for Selective Removal of Malachite Green. Water, Air, and Soil Pollution, 2015, 226, 1.	2.4	18
530	Fabrication of magnetic porous microspheres via (O 1 /W)/O 2 double emulsion for fast removal of Cu 2+ and Pb 2+. Journal of the Taiwan Institute of Chemical Engineers, 2016, 67, 505-510.	5.3	18
531	From adsorbents to electrode materials: facile hydrothermal synthesis of montmorillonite/polyaniline/metal oxide (hydroxide) composites. New Journal of Chemistry, 2016, 40, 2687-2695.	2.8	18
532	Sustainable Production of <i>o</i> â€Xylene from Biomassâ€Derived Pinacol and Acrolein. ChemSusChem, 2017, 10, 2880-2885.	6.8	18
533	Stable formamide/palygorskite nanostructure hybrid material fortified by high-pressure homogenization. Powder Technology, 2017, 318, 1-7.	4.2	18
534	Rapid nitrogen-rich modification of Calotropis gigantea fiber for highly efficient removal of fluoroquinolone antibiotics. Journal of Molecular Liquids, 2018, 256, 408-415.	4.9	18
535	Maximizing the Number of Interfacial Sites in Singleâ€Atom Catalysts for the Highly Selective, Solventâ€Free Oxidation of Primary Alcohols. Angewandte Chemie, 2018, 130, 7921-7925.	2.0	18
536	Cobalt-Doped Zinc Oxide Nanoparticle–MoS <sub>2</sub> Nanosheet Composites as Broad-Spectrum Bactericidal Agents. ACS Applied Nano Materials, 2021, 4, 4361-4370.	5.0	18
537	Synergy between Ru and WO <i><sub>x</sub></i> Enables Efficient Hydrodeoxygenation of Primary Amides to Amines. ACS Catalysis, 2022, 12, 6302-6312.	11.2	18
538	Superabsorbent composite. XIII. Effects of Al3+-attapulgite on hydrogel strength and swelling behaviors of poly(acrylic acid)/Al3+-attapulgite superabsorbent composites. Polymer Engineering and Science, 2007, 47, 619-624.	3.1	17
539	Adsorption of congo red onto lignocellulose/montmorillonite nanocomposite. Journal Wuhan University of Technology, Materials Science Edition, 2012, 27, 931-938.	1.0	17
540	Lanthanide complexes assembled from two flexible amide-type tripodal ligands: terminal groups effect on photoluminescence behavior. Dalton Transactions, 2012, 41, 3431.	3.3	17

#	Article	IF	CITATIONS
541	Removal of Cu <sup>2+</sup> and Zn <sup>2+</sup> Ions from Aqueous Solution Using Sodium Alginate and Attapulgite Composite Hydrogels. Adsorption Science and Technology, 2013, 31, 611-623.	3.2	17
542	Facile fabrication of well-defined polyaniline microtubes derived from natural kapok fibers for supercapacitors with long-term cycling stability. RSC Advances, 2016, 6, 68302-68311.	3.6	17
543	Water splitting: Taking cobalt in isolation. Nature Energy, 2016, 1, .	39.5	17
544	Crystal Plane Effect of ZnO on the Catalytic Activity of Gold Nanoparticles for the Acetylene Hydrogenation Reaction. Journal of Physical Chemistry C, 2017, 121, 19727-19734.	3.1	17
545	Making JPâ€10 Superfuel Affordable with a Lignocellulosic Platform Compound. Angewandte Chemie, 2019, 131, 12282-12286.	2.0	17
546	Hydrothermal Fabrication of Spindle-Shaped ZnO/Palygorskite Nanocomposites Using Nonionic Surfactant for Enhancement of Antibacterial Activity. Nanomaterials, 2019, 9, 1453.	4.1	17
547	The protective effects of modified palygorskite on the broilers fed a purified zearalenone-contaminated diet. Poultry Science, 2019, 98, 3802-3810.	3.4	17
548	Controllable fabrication of hierarchically porous adsorbent via natural particles stabilized Pickering medium internal phase emulsion for high-efficiency removal of Rb+ and Cs+. Journal of Cleaner Production, 2020, 277, 124092.	9.3	17
549	Protective effects of dietary supplementation with a silicate clay mineral (palygorskite) in lipopolysaccharide-challenged broiler chickens at an early age. Animal Feed Science and Technology, 2020, 263, 114459.	2.2	17
550	Preparation and properties of superabsorbent containing starch and sodium humate. Polymers for Advanced Technologies, 2008, 19, 1009-1014.	3.2	16
551	Study on superabsorbent composites. XVIII. Preparation, characterization, and property evaluation of poly(acrylic acidâ€ <i>co</i> â€acrylamide)/organomontmorillonite/sodium humate superabsorbent composites. Journal of Applied Polymer Science, 2008, 108, 211-219.	2.6	16
552	Effect of attapulgite contents on release behaviors of a pH sensitive carboxymethyl celluloseâ€ <i>g</i> â€poly(acrylic acid)/attapulgite/sodium alginate composite hydrogel bead containing diclofenac. Journal of Applied Polymer Science, 2012, 124, 4424-4432.	2.6	16
553	Facile preparation of stable palygorskite/cationic red X-GRL@SiO2"Maya Red―pigments. RSC Advances, 2014, 4, 63485-63493.	3.6	16
554	Palygorskite-based hybrid fluorescent pigment: Preparation, spectroscopic characterization and environmental stability. Microporous and Mesoporous Materials, 2016, 224, 107-115.	4.4	16
555	Solid Acid-Catalyzed Dehydration of Pinacol Derivatives in Ionic Liquid: Simple and Efficient Access to Branched 1,3-Dienes. ACS Catalysis, 2017, 7, 2576-2582.	11.2	16
556	Selective Cleavage of Câ^'O Bonds in Lignin Catalyzed by Rhenium(VII) Oxide (Re <sub>2</sub> O <sub>7</sub> ). ChemPlusChem, 2018, 83, 500-505.	2.8	16
557	An upgraded and universal strategy to reinforce chitosan/polyvinylpyrrolidone film by incorporating active silica nanorods derived from natural palygorskite. International Journal of Biological Macromolecules, 2020, 165, 1276-1285.	7.5	16
558	Incorporation of Lutein on Layered Double Hydroxide for Improving the Environmental Stability. Molecules, 2020, 25, 1231.	3.8	16

#	Article	IF	CITATIONS
559	Synergistic effect of palygorskite nanorods and ion crosslinking to enhance sodium alginate-based hydrogels. European Polymer Journal, 2021, 147, 110306.	5.4	16
560	Efficient Synthesis of Monomeric Fe Species in Zeolite ZSMâ€5 for the Lowâ€Temperature Oxidation of Methane. ChemCatChem, 2021, 13, 2766-2770.	3.7	16
561	Synthesis and application of eco-friendly superabsorbent composites based on xanthan gum and semi-coke. International Journal of Biological Macromolecules, 2021, 179, 230-238.	7.5	16
562	A comparative study on surface/interface mechanism and antibacterial properties of different hybrid materials prepared with essential oils active ingredients and palygorskite. Colloids and Surfaces A: Physicochemical and Engineering Aspects, 2021, 618, 126455.	4.7	16
563	Effectiveness evaluation of environmentally friendly stabilizers on remediation of Cd and Pb in agricultural soils by multi-scale experiments. Journal of Cleaner Production, 2021, 311, 127673.	9.3	16
564	Research on preparation and properties of a multifunctional superabsorbent based on semicoke and humic acid. European Polymer Journal, 2021, 159, 110750.	5.4	16
565	Multifunctional palygorskite@ZnO nanorods enhance simultaneously mechanical strength and antibacterial properties of chitosan-based film. International Journal of Biological Macromolecules, 2021, 189, 668-677.	7.5	16
566	Direct synthesis of a jet fuel range dicycloalkane by the aqueous phase hydrodeoxygenation of polycarbonate. Green Chemistry, 2021, 23, 3693-3699.	9.0	16
567	Study on superabsorbent composite. VIII. Effects of acid- and heat-activated attapulgite on water absorbency of polyacrylamide/attapulgite. Journal of Applied Polymer Science, 2007, 103, 2419-2424.	2.6	15
568	Promoting Role of Fe in the Preferential Oxidation of CO Over Ir/Al2O3. Catalysis Letters, 2008, 121, 319-323.	2.6	15
569	Rapid removal of Pb(II) from aqueous solution by chitosanâ€ <i>g</i> â€poly(acrylic) Tj ETQq1 1 0.784314 rgBT /v 2011, 32, 523-531.	Overlock 1 2.2	0 Tf 50 347 15
570	Effects of inorganic sulfates on the microstructure and properties of ion-exchange treated palygorskite clay. Colloids and Surfaces A: Physicochemical and Engineering Aspects, 2012, 405, 59-64.	4.7	15
571	Kapok fiber structure-oriented polyallylthiourea: Efficient adsorptive reduction for Au(III) for catalytic application. Polymer, 2014, 55, 5211-5217.	3.8	15
572	Palygorskite/polystyrene nanocomposites via facile in-situ bulk polymerization: Gelation and thermal properties. Applied Clay Science, 2014, 100, 95-101.	5.2	15
573	All-solid-state high-energy asymmetric supercapacitor based on natural tubular fibers. Journal of Materials Science, 2018, 53, 11659-11670.	3.7	15
574	A Convenient and Versatile Strategy for the Functionalization of Silica Foams Using High Internal Phase Emulsion Templates as Microreactors. ACS Applied Materials & Interfaces, 2020, 12, 14607-14619.	8.0	15
575	Photo–thermo Catalytic Oxidation over a TiO 2 â€WO 3 ‣upported Platinum Catalyst. Angewandte Chemie, 2020, 132, 13009-13016.	2.0	15

576 Synthesis, characterization, and swelling behaviors of sodium carboxymethyl cellulose-g-poly(acrylic) Tj ETQq0 0 0 rgBT /Overlock 10 Tf

#	Article	IF	CITATIONS
577	Preparation of Carboxymethyl Cellulose-g- Poly(acrylamide)/Attapulgite Porous Monolith With an Eco-Friendly Pickering-MIPE Template for Ce(III) and Gd(III) Adsorption. Frontiers in Chemistry, 2020, 8, 398.	3.6	15
578	Superabsorbent composite. X. Effects of saponification on properties of polyacrylamide/attapulgite. Polymer Engineering and Science, 2006, 46, 1762-1767.	3.1	14
579	Synthesis and swelling characteristics of a pHâ€responsive guar gumâ€ <i>g</i> â€poly(sodium) Tj ETQq1 1 0.7	784314 rgB 4.6	T /Overlock 1 14
580	pH-sensitive sodium alginate/calcined hydrotalcite hybrid beads for controlled release of diclofenac sodium. Drug Development and Industrial Pharmacy, 2012, 38, 728-734.	2.0	14
581	A pH-Sensitive Biopolymer-Based Superabsorbent Nanocomposite from Sodium Alginate and Attapulgite: Synthesis, Characterization, and Swelling Behaviors. Journal of Dispersion Science and Technology, 2012, 33, 1154-1162.	2.4	14
582	Preparation of manganese dioxide/multiwalled carbon nanotubes hybrid hollow microspheres via layer-by-layer assembly for supercapacitor. Journal of Materials Science, 2013, 48, 7581-7586.	3.7	14
583	Gum-g-Copolymers: Synthesis, Properties, and Applications. , 2013, , 149-203.		14
584	Influence of Anions on the Electrokinetic and Colloidal Properties of Palygorskite Clay via High-Pressure Homogenization. Journal of Chemical & Engineering Data, 2013, 58, 764-772.	1.9	14
585	Effect of squeeze, homogenization, and freezing treatments on particle diameter and rheological properties of palygorskite. Advanced Powder Technology, 2014, 25, 968-977.	4.1	14
586	From spent dye-loaded palygorskite to a multifunctional palygorskite/carbon/Ag nanocomposite. RSC Advances, 2016, 6, 41696-41706.	3.6	14
587	A comparative study on color properties of different clay minerals/BiVO4 hybrid pigments with excellent thermal stability. Applied Clay Science, 2019, 181, 105221.	5.2	14
588	Stabilization of GaAs photoanodes by <i>in situ</i> deposition of nickel-borate surface catalysts as hole trapping sites. Sustainable Energy and Fuels, 2019, 3, 814-822.	4.9	14
589	Fabrication of Eco-Friendly Superabsorbent Composites Based on Waste Semicoke. Polymers, 2020, 12, 2347.	4.5	14
590	Solid-phase oxalic acid leaching of natural red palygorskite-rich clay: A solvent-free way to change color and properties. Applied Clay Science, 2020, 198, 105848.	5.2	14
591	Synthesis, Crystal Structures, and Luminescent Properties of Noninterpenetrating (6,3) Type Network Lanthanide Metal–Organic Frameworks Assembled by a New Semirigid Bridging Ligand. European Journal of Inorganic Chemistry, 2010, 2010, 5318-5325.	2.0	13
592	Equilibrium isotherm and mechanism studies of Pb(II) and Cd(II) ions onto hydrogel composite based on vermiculite. Desalination and Water Treatment, 2012, 48, 38-49.	1.0	13
593	Preparation and Swelling Behavior of a pH-Responsive Psyllium- <i>g</i> -Poly(acrylic acid)/Attapulgite Superabsorbent Nanocomposite. International Journal of Polymeric Materials and Polymeric Biomaterials, 2012, 61, 906-918.	3.4	13
594	Nanocasting Synthesis of Mesostructured Co3O4 via a Supercritical CO2 Deposition Method and the Catalytic Performance for CO Oxidation. Catalysis Letters, 2012, 142, 275-281.	2.6	13

#	Article	IF	CITATIONS
595	Kinetic and Thermodynamic Studies on the Removal of Oil from Water Using Superhydrophobic Kapok Fiber. Water Environment Research, 2014, 86, 360-365.	2.7	13
596	Utilization of hollow kapok fiber for the fabrication of a pH-sensitive superabsorbent composite with improved gel strength and swelling properties. RSC Advances, 2014, 4, 50478-50485.	3.6	13
597	Synthesis of jet fuel rang cycloalkane from isophorone with glycerol as a renewable hydrogen source. Catalysis Today, 2017, 298, 16-20.	4.4	13
598	Effects of Dietary Synbiotic Supplementation as an Alternative to Antibiotic on the Growth Performance, Carcass Characteristics, Meat Quality, Immunity, and Oxidative Status of Cherry Valley Ducks. Journal of Poultry Science, 2018, 55, 182-189.	1.6	13
599	Zinc-loaded palygorskite nanocomposites for catheter coating with excellent antibacterial and anti-biofilm properties. Colloids and Surfaces A: Physicochemical and Engineering Aspects, 2020, 600, 124965.	4.7	13
600	A study on improving the antibacterial properties of palygorskite by using cobalt-doped zinc oxide nanoparticles. Applied Clay Science, 2021, 209, 106112.	5.2	13
601	Efficient Synthesis of Pharmaceutical Intermediates from Biomass-Derived Aldehydes and Ketones over Robust Ni <sub><i>x</i></sub> Al Nanocatalysts. ACS Sustainable Chemistry and Engineering, 2022, 10, 5526-5537.	6.7	13
602	Study on superabsorbent composite. XII. Effect of ion-exchanged attapulgite on water absorbency of poly(acrylic acid)/attapulgite superabsorbent composites. Journal of Applied Polymer Science, 2007, 105, 3476-3482.	2.6	12
603	Selective catalytic reduction of NO with propene over Au/CeO2/Al2O3 catalysts. Gold Bulletin, 2007, 40, 52-58.	2.7	12
604	Study on superabsorbent composite. XX. Effects of cationâ€exchanged montmorillonite on swelling properties of superabsorbent composite containing sodium humate. Polymer Composites, 2009, 30, 1138-1145.	4.6	12
605	Preparation and characterization of magnetic alginate-chitosan hydrogel beads loaded matrine. Drug Development and Industrial Pharmacy, 2012, 38, 872-882.	2.0	12
606	Ethanolâ€assisted dispersion of attapulgite and its effect on improving properties of alginateâ€based superabsorbent nanocomposite. Journal of Applied Polymer Science, 2013, 129, 1080-1088.	2.6	12
607	Effect of number of grindings of attapulgite on enhanced swelling properties of the superabsorbent nanocomposites. Journal of Composite Materials, 2013, 47, 969-978.	2.4	12
608	Development of a superporous hydroxyethyl celluloseâ€based hydrogel by anionic surfactant micelle templating with fast swelling and superabsorbent properties. Journal of Applied Polymer Science, 2015, 132, .	2.6	12
609	Facile fabrication of polyaniline/kapok fiber composites via a semidry method and application in adsorption and catalyst support. Cellulose, 2015, 22, 615-624.	4.9	12
610	Oriented Functionalization of Natural Hollow Kapok Fiber for Highly Efficient Removal of Toxic Hg(II) from Aqueous Solution. Frontiers in Environmental Science, 2016, 4, .	3.3	12
611	Selective Production of Toluene from Biomassâ€Đerived Isoprene and Acrolein. ChemSusChem, 2016, 9, 3434-3440.	6.8	12
612	Direct Synthesis of Renewable Dodecanol and Dodecane with Methyl Isobutyl Ketone over Dualâ€Bed Catalyst Systems. ChemSusChem, 2017, 10, 825-829.	6.8	12

#	Article	IF	CITATIONS
613	Morphology control of polyaniline by dopant grown on hollow carbon fibers as high-performance supercapacitor electrodes. Cellulose, 2017, 24, 5579-5592.	4.9	12
614	Continuous Carbon Hollow Shell with Zinc Oxide Nanoparticles Embedded as an Anode Material with Excellent Lithium Storage Capability. Energy Technology, 2018, 6, 188-195.	3.8	12
615	Effects of different pH regulators on the color properties of attapulgite/BiVO4 hybrid pigment. Powder Technology, 2019, 343, 68-78.	4.2	12
616	Synthesis of jet fuel range high-density dicycloalkanes with methyl benzaldehyde and acetone. Sustainable Energy and Fuels, 2020, 4, 5560-5567.	4.9	12
617	Sustainable Production of Safe Plasticizers with Bio-Based Fumarates and 1,3-Dienes. Industrial & Engineering Chemistry Research, 2020, 59, 7367-7374.	3.7	12
618	Potential of Phosphate Ion Removal Using an Al <sup>3+</sup> -Cross-linked Chitosan- <i>g</i> -Poly(Acrylic Acid)/Vermiculite Ionic Hybrid. Adsorption Science and Technology, 2010, 28, 89-99.	3.2	11
619	Dose–dependent biodistribution of prenatal exposure to rutile-type titanium dioxide nanoparticles on mouse testis. Journal of Nanoparticle Research, 2014, 16, 1.	1.9	11
620	Effects of Sodium Salts Organic Acids Modification on the Microstructure and Dispersion Behavior of Palygorskite Nano-Powder via High-Pressure Homogenization Process. Journal of Dispersion Science and Technology, 2014, 35, 840-847.	2.4	11
621	Halloysite nanotubes template-induced fabrication of carbon/manganese dioxide hybrid nanotubes for supercapacitors. Ionics, 2015, 21, 2329-2336.	2.4	11
622	CoAl2O4/Kaoline Hybrid Pigment Prepared via Solid-Phase Method for Anticorrosion Application. Frontiers in Chemistry, 2018, 6, 586.	3.6	11
623	Effects of different levels of modified palygorskite supplementation on the growth performance, immunity, oxidative status and intestinal integrity and barrier function of broilers. Journal of Animal Physiology and Animal Nutrition, 2018, 102, 1574-1584.	2.2	11
624	Potential of oxalic acid leached natural palygorskite-rich clay as multidimensional nanofiller to improve polypropylene. Powder Technology, 2022, 396, 456-466.	4.2	11
625	Palygorskite-Based Organic–Inorganic Hybrid Nanocomposite for Enhanced Antibacterial Activities. Nanomaterials, 2021, 11, 3230.	4.1	11
626	Preparation of efficient adsorbent with dual adsorption function based on semi-coke: Adsorption properties and mechanisms. Journal of Colloid and Interface Science, 2022, 626, 674-686.	9.4	11
627	Selective Catalytic Reduction of NO with CH4 Over In–Fe/Sulfated Zirconia Catalysts. Catalysis Letters, 2011, 141, 1491-1497.	2.6	10
628	Facile approach to magnetic attapulgite-Fe3O4/polystyrene tri-component nanocomposite. Materials Letters, 2012, 85, 11-13.	2.6	10
629	Adsorption/reaction energetics measured by microcalorimetry and correlated with reactivity on supported catalysts: A review. Chinese Journal of Catalysis, 2016, 37, 2039-2052.	14.0	10
630	Preparation of Chitosan-g-Poly (Vinylimidazole-co-2-Acrylamido-2-Methyl Propane Sulfonic Acid) Granular Hydrogel for Selective Adsorption of Hg2+. Water, Air, and Soil Pollution, 2016, 227, 1.	2.4	10

#	Article	IF	CITATIONS
631	Palygorskite Nanomaterials: Structure, Properties, and Functional Applications. , 2019, , 21-133.		10
632	Vermiculite Nanomaterials: Structure, Properties, and Potential Applications. , 2019, , 415-484.		10
633	Effects of palygorskite composites on growth performance and antioxidant status in broiler chickens. Poultry Science, 2019, 98, 2781-2789.	3.4	10
634	Production of 1,2-Cyclohexanedicarboxylates from Diacetone Alcohol and Fumarates. ACS Sustainable Chemistry and Engineering, 2019, 7, 2980-2988.	6.7	10
635	Preparation and Antibacterial Activity of ZnO/Palygorskite Nanocomposites Using Different Types of Surfactants. Journal of Inorganic and Organometallic Polymers and Materials, 2020, 30, 3808-3817.	3.7	10
636	Preparation of porous microspherical adsorbent via pine pollen stabilized O1/W/O2 double emulsion for high-efficient removal of cationic dyes. Colloids and Surfaces A: Physicochemical and Engineering Aspects, 2020, 601, 124997.	4.7	10
637	Removal of a cationic dye from aqueous solution by a porous adsorbent templated from eco-friendly Pickering MIPEs using chitosan-modified semi-coke particles. New Journal of Chemistry, 2021, 45, 3848-3856.	2.8	10
638	Zeoliteâ€Tailored Active Site Proximity for the Efficient Production of Pentanoic Biofuels. Angewandte Chemie, 2021, 133, 23906-23914.	2.0	10
639	Novel eco-friendly spherical porous adsorbent fabricated from Pickering middle internal phase emulsions for removal of Pb(II) and Cd (II). Journal of Environmental Sciences, 2022, 112, 320-330.	6.1	10
640	Preparation, characterization and performance evaluation of chitosan/palygorskite/glycyrrhizic acid nanocomposite films. Applied Clay Science, 2022, 216, 106322.	5.2	10
641	Synthesis of jet fuel range polycyclic alkanes and aromatics from furfuryl alcohol and isoprene. Green Chemistry, 2022, 24, 3130-3136.	9.0	10
642	Porous materials fabricated from Pickering foams stabilized by natural plant of Angelica sinensis for removal of Cd (II) and Cu (II). Colloids and Surfaces A: Physicochemical and Engineering Aspects, 2022, 648, 128695.	4.7	10
643	Eco-friendly superabsorbent composites based on calcined semicoke and polydimethylourea phosphate: Synthesis, swelling behavior, degradability and their impact on cabbage growth. Colloids and Surfaces A: Physicochemical and Engineering Aspects, 2022, 648, 129439.	4.7	10
644	Green synthesized Se–ZnO/attapulgite nanocomposites using Aloe vera leaf extract: Characterization, antibacterial and antioxidant activities. LWT - Food Science and Technology, 2022, 165, 113762.	5.2	10
645	Langmuir-Blodgett film of 1,3,6,11,13,18,28,31-octabromofullerene-C60. Thin Solid Films, 1994, 251, 4-6.	1.8	9
646	Study on superabsorbent composite. XV. Effects of ion-exchanged attapulgite on water absorbency of superabsorbent composites. Polymer Composites, 2007, 28, 208-213.	4.6	9
647	Study on superabsorbent composite XXV. Synthesis, characterization, and swelling behaviors of poly(acrylic acidâ€ <i>co</i> â€ <i>N</i> â€acryloylmorpholine)/attapulgite superabsorbent composites. Polymer Composites, 2010, 31, 691-699.	4.6	9
648	Glycine-assisted evolution of palygorskite via a one-step hydrothermal process to give an efficient adsorbent for capturing Pb( <scp>ii</scp> ) ions. RSC Advances, 2015, 5, 96829-96839.	3.6	9

#	Article	IF	CITATIONS
649	Thiourea-Induced Change Of Structure And Color Of Brick-Red Palygorskite. Clays and Clay Minerals, 2018, 66, 403-414.	1.3	9
650	Synthesis of palygorskite/polystyrene nanocomposites without crosslinked network via in-situ radical bulk polymerization technique. Applied Clay Science, 2018, 163, 273-278.	5.2	9
651	Insights into halloysite or kaolin role of BiVO4 hybrid pigments for applications in polymer matrix and surface coating. Composites Part B: Engineering, 2019, 174, 107035.	12.0	9
652	Comparative study on photocatalytic degradation of Congo red using different clay mineral/CdS nanocomposites. Journal of Materials Science: Materials in Electronics, 2019, 30, 5383-5392.	2.2	9
653	Fabrication of Eco-Friendly Betanin Hybrid Materials Based on Palygorskite and Halloysite. Materials, 2020, 13, 4649.	2.9	9
654	MIL-53 (Al) derived single-atom Rh catalyst for the selective hydrogenation of m-chloronitrobenzene into m-chloroaniline. Chinese Journal of Catalysis, 2021, 42, 824-834.	14.0	9
655	Size-Controlled Synthesis of CuO Nanoparticles by the Supercritical Antisolvent Method in SBA-15. ACS Sustainable Chemistry and Engineering, 2021, 9, 129-136.	6.7	9
656	Attapulgite: from clay minerals to functional materials. Scientia Sinica Chimica, 2018, 48, 1432-1451.	0.4	9
657	Recovering metal ions from oxalic acid leaching palygorskite-rich clay wastewater to fabricate layered mixed metal oxide/carbon composites for high-efficient removing Congo red. Chemosphere, 2022, 290, 132543.	8.2	9
658	Dietary palygorskite-based antibacterial agent supplementation as an alternative to antibiotic improves growth performance, intestinal mucosal barrier function, and immunity in broiler chickens. Poultry Science, 2022, 101, 101640.	3.4	9
659	Bio-template synthesis of three-dimensional microtubular nickel-cobalt layered double hydroxide composites for energy storage. Cellulose, 2018, 25, 4121-4131.	4.9	8
660	Polyaniline-functionalized porous adsorbent for Sr2+ adsorption. Journal of Radioanalytical and Nuclear Chemistry, 2018, 317, 907-917.	1.5	8
661	Controlling CO 2 Hydrogenation Selectivity by Metalâ€Supported Electron Transfer. Angewandte Chemie, 2020, 132, 20158-20164.	2.0	8
662	From the Waste Semicoke to Superabsorbent Composite: Synthesis, Characterization and Performance Evaluation. Journal of Polymers and the Environment, 2021, 29, 4017-4026.	5.0	8
663	Fast and Highly Efficient Adsorption Removal of Toxic Pb(II) by a Reusable Porous Semi-IPN Hydrogel Based on Alginate and Poly(Vinyl Alcohol). Frontiers in Chemistry, 2021, 9, 662482.	3.6	8
664	Preparation and coloring mechanism of MAl2O4/CoAl2O4/quartz sand (M = Ca or Ba) composite pigments. Materials Chemistry and Physics, 2022, 276, 125413.	4.0	8
665	Synergistic Effect of Glycyrrhizic Acid and ZnO/Palygorskite on Improving Chitosan-Based Films and Their Potential Application in Wound Healing. Polymers, 2021, 13, 3878.	4.5	8
666	Removal of Congo Red from Aqueous Solution by Sorption on Organified Rectorite. Clean - Soil, Air, Water, 2010, 38, 670-677.	1.1	7

#	Article	lF	CITATIONS
667	Swelling Behavior of Guar Gum-g-Poly(Sodium Acrylate -co-Styrene)/Attapulgite Superabsorbent Composites. Journal of Macromolecular Science - Physics, 2011, 50, 1847-1863.	1.0	7
668	Fabrication of stable glycine/palygorskite nanohybrid via high-pressure homogenization as high-efficient adsorbent for Cs(I) and methyl violet. Journal of the Taiwan Institute of Chemical Engineers, 2017, 80, 997-1005.	5.3	7
669	Selective Production of Renewable <i>para</i> â€Xylene by Tungsten Carbide Catalyzed Atomâ€Economic Cascade Reactions. Angewandte Chemie, 2018, 130, 1826-1830.	2.0	7
670	Preparation and oil absorbency of kapok- <i>g</i> -butyl methacrylate. Environmental Technology (United Kingdom), 2018, 39, 1089-1095.	2.2	7
671	Styrene Hydroformylation with In Situ Hydrogen: Regioselectivity Control by Coupling with the Lowâ€Temperature Water–Gas Shift Reaction. Angewandte Chemie, 2020, 132, 7500-7504.	2.0	7
672	The high-efficiency synergistic and broad-spectrum antibacterial effect of cobalt doped zinc oxide quantum dots (Co-ZnO QDs) loaded cetyltributylphosphonium bromide (CTPB) modified MMT (C-MMT) nanocomposites. Colloids and Surfaces A: Physicochemical and Engineering Aspects, 2021, 613, 126059.	4.7	7
673	Nanoscale Clay Minerals for Functional Ecomaterials: Fabrication, Applications, and Future Trends. , 2018, , 1-82.		7
674	Reduction of SO2 by CO under Plasma-assisted Catalytic System Induced by Microwave. Catalysis Letters, 2006, 109, 109-113.	2.6	6
675	Gold supported on surface acidity modified ZSM-5 for SCR of NO with propene. Reaction Kinetics and Catalysis Letters, 2007, 92, 33-39.	0.6	6
676	Utilization of plant ash for the fabrication of novel superabsorbent composites with potassiumâ€release characteristics. Journal of Applied Polymer Science, 2010, 115, 1814-1822.	2.6	6
677	Effect of Solvents Treatment on Microstructure and Dispersion Properties of Palygorskite. Journal of Dispersion Science and Technology, 2013, 34, 334-341.	2.4	6
678	Characterization and Congo Red uptake capacity of a new lignocellulose/organic montmorillonite composite. Desalination and Water Treatment, 2013, 51, 7120-7129.	1.0	6
679	Synthesis and enhanced photoelectric performance of Au/ZnO hybrid hollow sphere. RSC Advances, 2015, 5, 103636-103642.	3.6	6
680	Ru/H-beta as an efficient catalyst for the conversion of furfural into 3-acetyl-1-propanol (3-AP) toward one-pot transformation of xylan to 3-AP. Molecular Catalysis, 2019, 476, 110506.	2.0	6
681	Kinetic study of cellulose hydrolysis with tungstenâ€based acid catalysts. AICHE Journal, 2019, 65, e16585.	3.6	6
682	Polydopamine-clay functionalized <i>Calotropis gigantea</i> fiber: A recyclable oil-absorbing material with large lumens. Journal of Natural Fibers, 2019, 16, 1156-1165.	3.1	6
683	Highly efficient Co single-atom catalyst for epoxidation of plant oils. Journal of Chemical Physics, 2021, 154, 131103.	3.0	6
684	Development of porous material via chitosan-based Pickering medium internal phase emulsion for efficient adsorption of Rb+, Cs+ and Sr2+. International Journal of Biological Macromolecules, 2021, 193, 1676-1684.	7.5	6

#	Article	IF	CITATIONS
685	Synthesis of jet fuel range high-density polycycloalkanes with vanillin and cyclohexanone. Sustainable Energy and Fuels, 2022, 6, 1616-1624.	4.9	6
686	Incorporation of Different Metal Ion for Tuning Color and Enhancing Antioxidant Activity of Curcumin/Palygorskite Hybrid Materials. Frontiers in Chemistry, 2021, 9, 760941.	3.6	6
687	Preparation of pre-wetted underwater superoleophobic porous material from green water-based foam for oil–water separation. Journal of Materials Science, 2022, 57, 9172-9186.	3.7	6
688	Mechanochemical preparation of low-cost cobalt blue composite pigments with good color and acid resistance based on desert sands. Ceramics International, 2022, 48, 27182-27191.	4.8	6
689	Pd/Sulfated Alumina—A New Effective Catalyst for the Selective Catalytic Reduction of NO with CH <sub>4</sub> . Topics in Catalysis, 2004, 30/31, 103-105.	2.8	5
690	pH-Responsive Nanocomposites From Methylcellulose and Attapulgite Nanorods: Synthesis, Swelling and Absorption Performance on Heavy Metal Ions. Journal of Macromolecular Science - Pure and Applied Chemistry, 2012, 49, 306-315.	2.2	5
691	Water-dispersible and stable fluorescent Maya Blue-like pigments. RSC Advances, 2015, 5, 35010-35016.	3.6	5
692	A comparison study on the effects of dietary conventional and ultra-fine ground palygorskite supplementation on the growth performance and digestive function of broiler chickens. Applied Clay Science, 2019, 181, 105211.	5.2	5
693	Desorption-dominated synthesis of CuO/SBA-15 with tunable particle size and loading in supercritical CO <sub>2</sub> . Nanotechnology, 2020, 31, 095602.	2.6	5
694	Preparation of high-performance bismuth yellow hybrid pigments by doping with inorganic oxides. Powder Technology, 2020, 373, 411-420.	4.2	5
695	Regeneration and Recycling of Spent Bleaching Earth. , 2019, , 3147-3167.		5
696	Nanoscale Clay Minerals for Functional Ecomaterials: Fabrication, Applications, and Future Trends. , 2019, , 2409-2490.		5
697	Facile fabrication of the porous adsorbent from natural plant Angelica Sinensis stabilized liquid foam for dye removal. Green Chemical Engineering, 2022, 3, 83-91.	6.3	5
698	Synthesis of renewable alkylated decalins with <i>p</i> -quinone and 2-methyl-2,4-pentanediol. Sustainable Energy and Fuels, 2022, 6, 834-840.	4.9	5
699	Semi-coke-enhanced eco-friendly superabsorbent composites for agricultural application. Polymer Bulletin, 2023, 80, 569-588.	3.3	5
700	Study of bubble behavior in high-viscosity liquid in a pseudo-2D column using high-speed imaging. Chemical Engineering Science, 2022, 252, 117532.	3.8	5
701	Structural Evolution of Palygorskite as the Nanocarrier of Silver Nanoparticles for Improving Antibacterial Activity. ACS Applied Bio Materials, 2022, 5, 3960-3971.	4.6	5
702	Adsorption of Congo Red by Poly(Dimethyl Diallyl Ammonium Chloride)/Polyacrylamide Hydrogels with Excellent Acid and Alkali Resistance. Separation Science and Technology, 2012, 47, 1828-1836.	2.5	4

#	Article	lF	CITATIONS
703	Kapok Fiber: Applications. , 2014, , 251-266.		4
704	Evolution of Fe3+-hydrogel for catalytic reduction of 4-nitrophenol. Colloid and Polymer Science, 2015, 293, 2009-2016.	2.1	4
705	Fabrication and Applications of Carbon/Clay Mineral Nanocomposites. , 2019, , 537-587.		4
706	Synthesis of renewable aviation fuel additives with aromatic aldehydes and methyl isobutyl ketone under solvent-free conditions. Sustainable Energy and Fuels, 2021, 5, 556-563.	4.9	4
707	FABRICATION OF ANTHOCYANIN/MONTMORILLONITE HYBRID PIGMENTS TO ENHANCE THEIR ENVIRONMENTAL STABILITY AND APPLICATION IN ALLOCHROIC COMPOSITE FILMS. Clays and Clay Minerals, 2021, 69, 142-151.	1.3	4
708	An Evaluation of the Supplementation of Dietary-Modified Palygorskite on Growth Performance, Zearalenone Residue, Serum Metabolites, and Antioxidant Capacities in Broilers Fed a Zearalenone-Contaminated Diet. Clays and Clay Minerals, 2018, 66, 474-484.	1.3	4
709	Synthesis of jet fuel and diesel range cycloalkanes with 2-methylfuran and benzaldehyde. Sustainable Energy and Fuels, 2022, 6, 1156-1163.	4.9	4
710	Improved structural and catalytic attributes of Ba2Co2Fe12â^'2x(Zr,Ni)xO22 materials synthesized by sol–gel and microwave heating methods. Journal of Materials Chemistry, 2012, 22, 22190.	6.7	3
711	A pH sensitive carboxymethyl cellulose- g -poly (acrylic acid)/polyvinylpyrrolidone/sodium alginate composite hydrogel bead for the controlled release of diclofenac. Journal of Controlled Release, 2015, 213, e91-e92.	9.9	3
712	Amino-acid-assisted preparation of CoAl2O4/kaolin hybrid pigments. Applied Clay Science, 2020, 191, 105611.	5.2	3
713	EFFECTS OF DIETARY PALYGORSKITE SUPPLEMENTATION ON CECAL MICROBIAL COMMUNITY STRUCTURE AND THE ABUNDANCE OF ANTIBIOTIC-RESISTANT GENES IN BROILER CHICKENS FED WITH CHLORTETRACYCLINE. Clays and Clay Minerals, 2021, 69, 205-216.	1.3	3
714	Calcined Oil Shale Semi-coke for Significantly Improved Performance Alginate-Based Film by Crosslinking with Ca2+. Journal of Polymers and the Environment, 2022, 30, 2405-2418.	5.0	3
715	Facile mechanochemical fabrication of hybrid pigments with allochroic, antibacterial and superhydrophobic properties based on organo-palygorskite and curcumin. Dyes and Pigments, 2022, 203, 110359.	3.7	3
716	CaCO3-assisted mechanochemical synthesis of low-cost and high-chroma cobalt blue composite pigments using kaolin tailing sand for ceramic coloring. Journal of Industrial and Engineering Chemistry, 2022, 112, 440-450.	5.8	3
717	Utilization of Sea Sand for Preparation of High-Performance CoAl <sub>2</sub> O <sub>4</sub> Composite Pigments <i>via</i> a Cleaner Mechanochemistry Route. ACS Sustainable Chemistry and Engineering, 2022, 10, 9553-9564.	6.7	3
718	Effects of {2-[(3-carboxy-1-oxoprogy1)amino]-2-deoxy-D-glucose} on human hepatocellular carcinoma cell line. Acta Pharmacologica Sinica, 2005, 26, 635-640.	6.1	2
719	Promotional role of CeO2 in reduction of NO with activated carbon under oxygen-rich atmosphere. Topics in Catalysis, 2007, 42-43, 263-266.	2.8	2
720	Cover Picture: Direct Catalytic Conversion of Cellulose into Ethylene Glycol Using Nickel-Promoted Tungsten Carbide Catalysts (Angew. Chem. Int. Ed. 44/2008). Angewandte Chemie - International Edition, 2008, 47, 8321-8321.	13.8	2

#	ARTICLE	IF	CITATIONS
721	Study on superabsorbent composites XVII. Preparation and characterization of poly(acrylic) Tj ETQq1 1 0.784314	rgBT	Overlock 10 Ti
722	Aberration-corrected STEM Study of Atomically Dispersed Pti/FeOx Catalyst with High Loading of Pt. Microscopy and Microanalysis, 2015, 21, 1733-1734.	0.4	2
723	One-pot preparation of superparamagnetic attapulgite/Fe3O4/polydopamine nanocomposites for adsorption of methylene blue. AIP Conference Proceedings, 2016, , .	0.4	2
724	Investigation on the Effect of Poly(butylmethacrylate)/attapulgite Nanocomposites for Oil Absorption. Water Environment Research, 2016, 88, 1994-2000.	2.7	2
725	Evaluation of palygorskite on pellet quality, growth, antioxidant status and mineral contents of Chinese mitten crabs ( Eriocheir sinensis ). Aquaculture Research, 2020, 51, 1446-1454.	1.8	2
726	Capturing the flow field of bubbly flows using BTV in high viscosity liquid. Chemical Engineering Science, 2020, 227, 115943.	3.8	2
727	Magnetic Halloysite/Fe3O4/AuNPs Nanocomposite as a Recyclable Efficient Catalyst for Hydrogenation of Congo Red and 4-Nitrophenol. Current Environmental Engineering, 2018, 5, 144-154.	0.6	2
728	W/O HIPEs templated polyaniline/polystyrene porous adsorbent for Sr2+ uptake from aqueous solution. , 0, 132, 99-108.		2
729	Regeneration and Recycling of Spent Bleaching Earth. , 2018, , 1-21.		2
730	Mechanochemical synthesis of multifunctional kaolin@ <scp>BiVO<sub>4</sub></scp> hybrid pigments for coloring and reinforcing of acrylonitrileâ€butadieneâ€styrene. Journal of Applied Polymer Science, 2022, 139, .	2.6	2
731	Preparation and Properties of Antibacterial Polyhexamethylene Biguanide/Palygorskite Composites as Zearalenone Adsorbents. Clays and Clay Minerals, 0, , 1.	1.3	2
732	Facile Preparation of Organo-Modified ZnO/Attapulgite Nanocomposites Loaded with Monoammonium Glycyrrhizinate via Mechanical Milling and Their Synergistic Antibacterial Effect. Minerals (Basel,) Tj ETQq0 0 0 rgf	3T2/QV(	erlock210 Tf 50 2
733	Preparation, Characterization and Swelling Behaviours of a Novel Multifunctional Superabsorbent Composite Based on Ca-Montmorillonite and Sodium Humate. E-Polymers, 2007, 7, .	3.0	1
734	Rücktitelbild: Hydroformylation of Olefins by a Rhodium Single-Atom Catalyst with Activity Comparable to RhCl(PPh3 )3 (Angew. Chem. 52/2016). Angewandte Chemie, 2016, 128, 16412-16412.	2.0	1
735	Synthesis of Branched Octahydro-Indene with Methyl Benzaldehyde and Methyl Isobutyl Ketone. ACS Sustainable Chemistry and Engineering, 0, , .	6.7	1
736	Advanced Magnetic Adsorbents Prepared from Emulsion Template for Water Treatment. Environmental Chemistry for A Sustainable World, 2021, , 385-433.	0.5	1
737	High-capacity adsorption of cationic dyes using porous magnetic adsorbent. , 0, 118, 314-325.		1
738	Production of Copolyester Monomers from Plantâ€Based Acrylate and Acetaldehyde. Angewandte Chemie - International Edition, 2022, 61, .	13.8	1

#	Article	IF	CITATIONS
739	Structural evolution of palygorskite for reinforcing the performance of polypropylene. Composite Interfaces, 0, , 1-19.	2.3	1
740	Slow Release and Water Retention Performance of Poly(acrylic acid-co-acrylamide)/Fulvic Acid/Oil Shale Semicoke Superabsorbent Composites. Polymers, 2022, 14, 1719.	4.5	1
741	Biomediated synthesis of ZnO quantum dots decorated attapulgite nanocomposites for improved antibacterial properties. Green Processing and Synthesis, 2022, 11, 582-594.	3.4	1
742	Titelbild: Direct Catalytic Conversion of Cellulose into Ethylene Glycol Using Nickel-Promoted Tungsten Carbide Catalysts (Angew. Chem. 44/2008). Angewandte Chemie, 2008, 120, 8445-8445.	2.0	0
743	{2-[(3-Carboxy-1-oxopropyl) amino]-2-deoxy-d-Glucose} suppresses proliferation and induces apoptosis in the human esophageal cancer cell line. Medical Oncology, 2011, 28, 986-990.	2.5	0
744	Rücktitelbild: Catalytically Active Rh Subâ€Nanoclusters on TiO <sub>2</sub> for CO Oxidation at Cryogenic Temperatures (Angew. Chem. 8/2016). Angewandte Chemie, 2016, 128, 2998-2998.	2.0	0
745	Reply to "Comment to the paper: Effect of grinding time on fabricating a stable methylene blue/palygorskite hybrid nanocomposite, by Yuan Zhang, Wenbo Wang, Bin Mu, Qin Wang, Aiqin Wang― [Powder Technol. 280 (2015) 173–179]. Powder Technology, 2016, 299, 261-262.	4.2	0
746	Selective Cleavage of Câ^'O Bonds in Lignin Catalyzed by Rhenium(VII) Oxide (Re2 O7 ). ChemPlusChem, 2018, 83, 479-479.	2.8	0
747	Carbon Composites: Superamphiphobic Coatings with Low Sliding Angles from Attapulgite/Carbon Composites (Adv. Mater. Interfaces 9/2018). Advanced Materials Interfaces, 2018, 5, 1870045.	3.7	0
748	Synthesis of renewable alkylated naphthalenes with benzaldehyde and angelica lactone. Green Chemistry, 2021, 23, 5474-5480.	9.0	0
749	Facile fabrication of a stable fluorescent yellow X-10GFF/palygorskite hybrid pigment <i>via</i> semi-dry grinding. Clay Minerals, 2021, 56, 37-45.	0.6	0
750	Production of Copolyester Monomers from Plantâ€Based Acrylate and Acetaldehyde. Angewandte Chemie, 0, , .	2.0	0